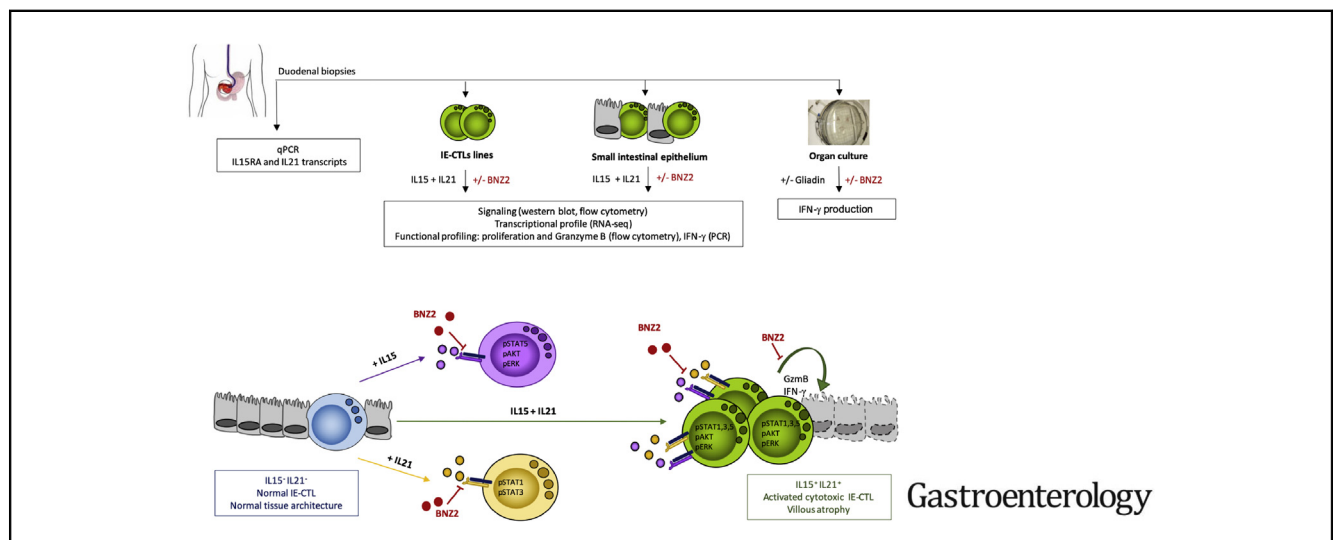




Identification of a γ c Receptor Antagonist That Prevents Reprogramming of Human Tissue-resident Cytotoxic T Cells by IL15 and IL21

Cezary Ciszewski,^{1,*} Valentina Discepolo,^{1,*} Alain Pacis,² Nick Doerr,³ Olivier Tastet,² Toufic Mayassi,^{1,4} Mariantonia Maglio,⁵ Asjad Basheer,³ Laith Q. Al-Mawsawi,³ Peter H. R. Green,⁶ Renata Auricchio,⁵ Riccardo Troncone,⁵ Thomas A. Waldmann,⁷ Nazli Azimi,³ Yutaka Tagaya,⁸ Luis B. Barreiro,^{1,9} and Bana Jabri^{1,4,10}

¹Department of Medicine, University of Chicago, Chicago, Illinois; ²Department of Genetics, CHU Sainte-Justine Research Center, Montreal, Quebec, Canada; ³Bioniz Therapeutics, Inc., Irvine, California; ⁴Committee on Immunology, University of Chicago, Chicago, Illinois; ⁵Department of Translational Medical Science and European Laboratory for the Investigation of Food Induced Diseases (ELFID), Università degli Studi di Napoli Federico II, Napoli, Italy; ⁶Celiac Disease Center, Columbia University, New York, New York; ⁷Lymphoid Malignancies Branch, National Cancer Institute, Bethesda, Maryland; ⁸Institute of Human Virology, University of Maryland School of Medicine, Baltimore, Maryland; ⁹Committee on Genetics, Genomics and Systems Biology, University of Chicago, Chicago, Illinois; and ¹⁰Department of Pathology and Pediatrics, University of Chicago, Chicago, Illinois



BACKGROUND & AIMS: Gamma chain (γ c) cytokines (interleukin [IL]2, IL4, IL7, IL9, IL15, and IL21) signal via a common γ c receptor. IL2 regulates the immune response, whereas IL21 and IL15 contribute to development of autoimmune disorders, including celiac disease. We investigated whether BNZ-2, a peptide designed to inhibit IL15 and IL21, blocks these cytokines selectively and its effects on intraepithelial cytotoxic T cells. **METHODS:** We obtained duodenal biopsies from 9 patients with potential celiac disease (positive results from tests for anti-TG2 but no villous atrophy), 30 patients with untreated celiac disease (with villous atrophy), and 5 patients with treated celiac disease (on a gluten-free diet), as well as 43 individuals without celiac disease (controls). We stimulated primary intestinal intraepithelial CD8⁺ T-cell lines, or CD8⁺ T cells directly isolated from intestinal biopsies, with γ c cytokines in presence or absence of BNZ-2. Cells were analyzed by immunoblots, flow cytometry, or RNA-sequencing analysis for phosphorylation of signaling molecules, gene expression

profiles, proliferation, and levels of granzyme B. **RESULTS:** Duodenal tissues from patients with untreated celiac disease had increased levels of messenger RNAs encoding IL15 receptor subunit alpha (IL15RA) and IL21 compared with tissues from patients with potential celiac disease and controls. Activation of intraepithelial cytotoxic T cells with IL15 or IL21 induced separate signaling pathways; incubation of the cells with IL15 and IL21 cooperatively increased their transcriptional activity, proliferation, and cytolytic properties. BNZ-2 specifically inhibited the effects of IL15 and IL21, but not of other γ c cytokines. **CONCLUSIONS:** We found increased expression of IL15RA and IL21 in duodenal tissues from patients with untreated celiac disease compared with controls. IL15 and IL21 cooperatively activated intestinal intraepithelial cytotoxic T cells. In particular, they increased their transcriptional activity, proliferation, and cytolytic activity. The peptide BNZ-2 blocked these effects, but not those of other γ c cytokines, including IL2. BNZ-2 might be used to prevent cytotoxic

T-cell-mediated tissue damage in complex immune disorders exhibiting upregulation of IL15 and IL21.

Keywords: Autoimmunity; Immune Response; Treatment; Signal Transduction.

The common gamma chain (γ c) cytokine family includes 6 members, interleukin (IL)-2, 4, 7, 9, 15, and 21, displaying a similar 4-helical bundle structure and sharing the common γ c receptor signaling subunit.¹ These cytokines are critically implicated both in immune homeostasis and immunopathology. IL15 and IL21 play a key role in the pathogenesis of organ-specific autoimmune and autoimmune-like disorders, such as type-1 diabetes,^{2,3} graft-versus-host disease,^{4,5} and celiac disease.^{6,7} IL2 is a pivotal cytokine for T-cell differentiation and activation.⁸ Despite signaling through the same receptor (IL2/IL15R $\beta\gamma$),⁹ IL2 and IL15 have distinct roles in vivo, with IL15 overexpression being associated with autoimmunity, and IL2 playing a critical immunoregulatory role by ensuring survival and expansion of regulatory T cells.¹⁰

Celiac disease is an immune-mediated disorder triggered by dietary gluten in genetically susceptible individuals. Small intestinal enteropathy in celiac disease is promoted by a crosstalk between epithelial stress signals associated with IL15 upregulation and an anti-gluten CD4⁺ T-cell response.¹¹ These 2 events are required for the licensing of intraepithelial cytotoxic T cells (IE-CTLs), responsible for tissue destruction.⁶ Importantly, IL21, produced by gluten-specific T cells,¹² enhances the adaptive immune response and contributes to interferon- γ (IFN- γ) production in active celiac disease.⁷ On a milder side of disease spectrum, potential celiac disease is characterized by the development of anti-gluten immunity in the absence of tissue damage. Importantly neither IL15¹¹ nor IL21¹³ were upregulated in potential celiac disease, suggesting they could play a role in villous atrophy. Whether both cytokines are coexpressed in active celiac disease and cooperate to activate human IE-CTL remains to be established. In line with this hypothesis, IL15 and IL21 synergistically promoted proliferation and effector function of murine CTL in vitro.¹⁴

A life-long gluten-free diet (GFD) is currently the only effective treatment for celiac disease; however, poor adherence and decreased quality of life have been reported. Furthermore, up to 30% of adult patients do not fully respond to gluten withdrawal¹⁵ and 1% to 2% develop refractory celiac disease (RCD), a precancerous condition.¹⁶ Thus, the need for alternative treatments for patients who fail to heal on a GFD.

In complex inflammatory disorders, like celiac disease, more than a single cytokine is often implicated in the immune response, thus the lack of full therapeutic efficacy of monoclonal antibodies. To address this concern, a novel multi-cytokine pharmacological inhibition approach has been recently proposed. Taking advantage of the structural information on the cytokine binding site on the γ c, multi γ c-cytokine inhibitors have been designed.¹⁷ The leading peptide, BNZ-1, safely and selectively blocked IL2, IL9, and IL15 signaling¹⁸ in the context

WHAT YOU NEED TO KNOW

BACKGROUND AND CONTEXT

Interleukin 2 (IL2) regulates the immune response, whereas IL21 and IL15 contribute to the development of autoimmune disorders, including celiac disease. We investigated whether BNZ-2, a peptide designed to inhibit IL15 and IL21, blocks these cytokines selectively and its effects on intraepithelial cytotoxic T cells.

NEW FINDINGS

We found increased expression of IL15RA and IL21 in duodenal tissues from patients with untreated celiac disease compared with controls. Incubation of intraepithelial cytotoxic T cells with IL15 or IL21 increased their proliferation and cytolytic activity, and the peptide BNZ-2 specifically blocked these effects, but not effects of IL2.

LIMITATIONS

This study was performed using cell lines and intraepithelial cytotoxic T cells isolated from duodenal biopsies. Further studies are needed in patients.

IMPACT

BNZ-2 might be used to prevent cytotoxic T-cell mediated damage to the intestinal mucosa in patients with immune regulatory disorders associated with overexpression of IL15 and IL21.

of T-cell malignancies¹⁹ in which both IL2 and IL15 have been implicated in driving the expansion and survival of malignant CTL. A second peptide, BNZ-2, designed to selectively block IL15 and IL21, has been synthesized, but its ability to inhibit IL15 and IL21 without hampering signaling of other γ c cytokines in human CTL remains to be determined.

In this study, we investigated the combined impact of IL15 and IL21 on signaling, transcription, and function of human tissue-resident IE-CTL both in vitro and ex vivo and tested in a preclinical setting the ability of BNZ-2 to selectively and concomitantly block IL15 and IL21.

Materials and Methods

Patients

Eighty-seven individuals undergoing esophago-gastro-duodenal endoscopy during diagnostic workup were enrolled from 3 centers: University of Chicago Medicine, Celiac Disease

* Authors share co-first authorship

Abbreviations used in this paper: AKT, protein kinase B; CP, control peptide; CTL, cytotoxic T lymphocytes; DEGs, differentially expressed genes; EC₅₀, half maximal effective concentration; ERK, extracellular signal-regulated kinase; FDR, false discovery rate; GFD, gluten free diet; IE-CTL, intraepithelial cytotoxic T lymphocytes; IELs, intraepithelial lymphocytes; Ig, immunoglobulin; IL, interleukin; IFN- γ , interferon gamma; NK, natural killer; qPCR, quantitative polymerase chain reaction; RNA-seq, RNA-sequencing; RCD, refractory celiac disease; STAT, signal transducer and activator of transcription; TG2, tissue transglutaminase; WB, western blot; γ c, gamma chain.

 Most current article

© 2020 by the AGA Institute
0016-5085/\$36.00

<https://doi.org/10.1053/j.gastro.2019.10.006>

Center at Columbia University, and Department of Pediatrics, University of Naples Federico II. Forty-three controls, 9 potential, 30 untreated, and 5 treated patients with celiac disease have been included (Supplementary Table 1). For each subject, 4 to 6 biopsies were obtained from the duodenum. Control subjects underwent esophago-gastro-duodenal-endoscopy during diagnostic workup about abdominal discomfort, failure to thrive, or other intestinal disorders unrelated to celiac disease. They all had normal duodenal histology, no family history of celiac disease, normal serum levels of anti-tissue transglutaminase (anti-TG2) immunoglobulin (Ig)A. Potential patients had positive anti-TG2 and no villous atrophy (histological Marsh score of 0–1). Untreated (or active) patients with celiac disease had positive anti-TG2 IgA and an enteropathy with increased intraepithelial lymphocytes (IEL), crypts hyperplasia, and villous atrophy, according to current diagnostic guidelines.^{15,20} Treated patients with celiac disease were on a GFD for at least 6 months and had normal duodenal histology and serum anti-TG2 IgA levels. Analysis of patient samples was approved by the Institutional Review Board of the University of Chicago (IRB-12623B), Columbia University (IRB-AAAB2472), and University of Naples Federico II (CE 230/05).

Cytokine and BNZ-2 Stimulation

CD8⁺ T-cell lines or ex vivo single-cell suspensions from the epithelial compartment (obtained as described in the Supplementary Methods) were stimulated with human recombinant IL15 (Biolegend, San Diego, CA), IL21 (Biolegend), or IL2 (NIH AIDS Reagent Program) at the indicated concentrations for 20 minutes for signaling experiments, western blot (WB), and flow cytometry, or 2 hours for RNA-sequencing (RNA-seq). BNZ-2, or a control peptide (CP), scrambled sequence of BNZ-2, was added at the indicated concentrations 10 minutes before cytokine stimulation.

Additional details are in the Supplementary Materials and Methods section.

Results

Concomitant Expression of IL15 and IL21 Is Associated With Intestinal Damage in Celiac Disease

IL15 and IL21 were both proven to promote cytolytic activity in CTLs.¹⁴ Their expression in the intestinal mucosa of patients with celiac disease was individually investigated.^{10,13,21–23} However, whether the 2 cytokines are coexpressed or define 2 distinct subsets of patients with celiac disease is unknown. To address this question, we analyzed transcript levels of IL21 and IL15 private receptor alpha, which is required for IL15 trans-presentation and signaling,²⁴ in the duodenum of subjects with celiac disease and controls. *IL15RA* and *IL21* transcripts were concomitantly overexpressed in 57.1% of active, but absent in patients with potential celiac disease (Figure 1A). Among patients with active celiac disease, 4.8% overexpressed only *IL21*, 9.5% only *IL15RA*, and one-third (28.6%) displayed neither IL15 nor IL21 upregulation.

In conclusion, selective upregulation of IL15 takes place in fewer than 10% of patients with active celiac disease, with

IL15 and/or IL21 expression being dysregulated in more than 71% and a large majority of patients with active celiac disease overexpressing both cytokines. Upregulation of IL15 and IL21 occurring only in active but in none of potential patients with celiac disease, suggests that these 2 cytokines could cooperatively contribute to tissue damage in celiac disease.

BNZ-2 Blocks the Signaling Pathways Enhanced by IL15 and IL21 in Tissue-resident IE-CTL

BNZ-2 is a novel γ c-binding peptide designed to specifically antagonize IL15 and IL21, but not the other members of the γ c-cytokine family.¹⁷ Its 21 amino-acid sequence, disclosed here for the first time, includes IL15- and IL21-specific, as well as shared residues (Figure 1B).

IE-CTL are the critical effector cells mediating epithelial destruction in celiac disease.^{25,26} To test the hypothesis that IL15 and IL21 cooperatively contribute to IE-CTL activation and that this could be blocked by BNZ-2, we treated human IE-CTL short-term cell lines with IL15 and IL21, in presence and absence of BNZ-2. These cell lines were generated from small intestinal CD45⁺CD103⁺CD3⁺CD8⁺TcR $\alpha\beta$ ⁺ IEL (Supplementary Figure 1). Phosphorylation at key residues was assessed by WB (Supplementary Figure 2) for signal transducer and activator of transcription (STAT) molecules, including STAT1 (pY701), STAT3 (pY705), and STAT5 (pY694), as well as protein kinase B (AKT, pS473), and extracellular signal-regulated kinase (ERK, pT202/Y204) in response to increasing concentrations of IL15 and IL21. In line with studies in human and mouse lymphocytes,^{27–31} we found that IL15 induced pSTAT5 and pERK in human IE-CTL in a dose-dependent manner starting at concentrations as low as 5 pM, whereas phosphorylation of STAT1 and AKT required at least 140 pM of IL15 (Supplementary Figure 2). In contrast to previous reports in peripheral blood lymphocytes²⁷ and NK cells,³⁰ but in agreement with what was demonstrated in CD4⁺ T cells,³¹ IL15 was overall ineffective at inducing pSTAT3 in IE-CTL: concentrations above 700 pM were required to observe STAT3 phosphorylation. On the other hand, in accordance with previous studies,³² IL21 promoted pSTAT1 and pSTAT3 starting at concentrations as low as 5 pM (Supplementary Figure 2); however, it failed to induce phosphorylation of STAT5, AKT and ERK even at high concentrations. Based on these results in human IE-CTL, we used concentrations of IL15 (140 pM) and IL21 (5 and 14 pM) that induced submaximal levels of pSTAT molecules to investigate whether they could have additive and/or synergistic effects (Figure 1C–E). A clear additive effect was observed for pSTAT1 on stimulation with IL21+IL15 compared with IL21 alone ($P < .05$, Figure 1D). The increase in pSTAT3 remained overall solely driven by IL21 (Figure 1D), whereas phosphorylation of STAT5, AKT, and ERK were induced selectively by IL15 (Figure 1E).

We next tested the ability of BNZ-2 to impair IL15 and IL21 signaling alone (Supplementary Figure 3) and in combination in human IE-CTL (Supplementary Figure 4 and Figure 1F). BNZ-2 efficiently blocked IL21-mediated phosphorylation of STAT1 ($P = .01$) and STAT3 ($P = .03$) (Supplementary Figure 3A), and IL15-induced

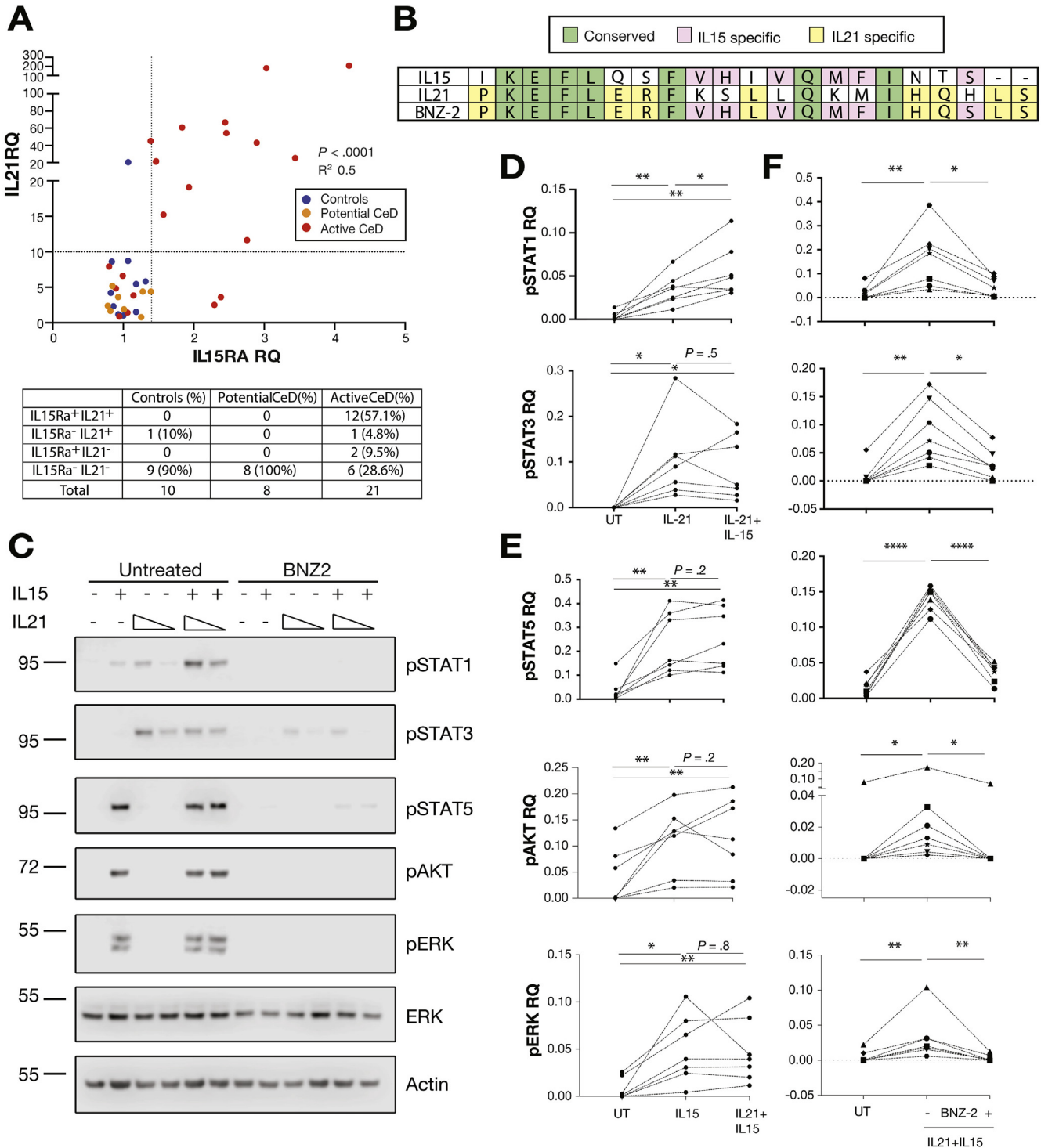


Figure 1. IL15 and IL21 are concomitantly upregulated in full-blown celiac disease and BNZ-2 impairs their cooperative signaling in human tissue-resident IE-CTL. (A) Relative quantification (RQ) of IL15 receptor alpha (*IL15RA*) and *IL21* transcripts levels in duodenal biopsies of 10 controls (blue), 8 patients with potential (orange), and 21 patients with active (red) celiac disease, as assessed by Taqman PCR. Two dotted lines indicate the cutoff used to define positive vs negative subjects. Number and percentages of patients in each quadrant are displayed in the table. *IL15RA* and *IL21* correlation was assessed by Pearson's test, $P < .0001$, $R^2 = 0.5$. (B) Alignment of the amino-acid sequences of the D-helices of IL15 (NP_000576.1, 144–162) and IL21 (NP_068575.1, 133–153) and BNZ-2. Conserved positions are in green, IL15 specific in pink, IL21 specific in yellow, unique residues in white. (C) One representative blot displaying pSTAT1, pSTAT3 and pSTAT5, pAKT and pERK in human IE-CTL lines in response to IL15 (140 pM) and IL21 (4 and 14 pM) in absence (left) or presence (right) of BNZ-2 (3 μ M). (D, E) Quantification by densitometry of 7 WB for pSTAT1 and pSTAT3 (D) on stimulation with IL21 (14 pM) alone or in combination with IL15 and pSTAT1, pAKT, and pERK (E) on stimulation with IL15 alone or in combination with IL21 (14 pM). (F) Quantification of 7 WB displaying levels of pSTAT1, pSTAT3, pSTAT5, pAKT, and pERK in response to IL15 (140pM) + IL21 (14 pM) in absence or presence of 3 μ M BNZ-2. (D–F) Phospho-protein levels are normalized to averaged ERK and actin total protein levels for each condition. Paired 1-way analysis of variance was performed, * $P < .05$.

phosphorylation of STAT5 ($P = .01$), AKT ($P = .002$), and ERK ($P = .003$) (Supplementary Figure 3B). More importantly, BNZ-2, but not its scrambled sequence used as a control, inhibited the combined activation of IE-CTL by IL15 and IL21 (Figure 1F and Supplementary Figure 4).

Altogether, these results indicate that in human tissue-resident IE-CTL stimulation with IL15 and IL21 results in the merger of their distinct individual signaling pathways, suggesting that they do not substitute for each other. Furthermore, we identify a new molecule, BNZ-2, that effectively blocks the signaling promoted by each (Supplementary Figure 3) and both (Figure 1F and Supplementary Figure 4) cytokines.

IL21 Further Modulates IL15 Driven Transcriptional Program in Tissue-resident IE-CTL

Prompted by the evidence that IL15 and IL21 induce a combined signaling profile in human IE-CTL that could not be triggered by them individually, we next investigated the impact of these cytokines on the transcriptional program of IE-CTL by RNA-seq. IE-CTL were stimulated with increasing doses of IL15 and IL21 to assess by quantitative polymerase chain reaction (qPCR) the half maximal effective concentration (EC_{50}) for the induction of granzyme B (GzmB) (Supplementary Figure 5A and B), a key mediator of cytotoxicity in CTL that is transcriptionally upregulated by both cytokines.³³ The EC_{50} for IL15 (700 pM) and IL21 (20 pM) was further confirmed by analyzing STAT3 and TNFS10 transcripts (Supplementary Figure 5A and B). RNA-seq analysis of 7 IE-CTL lines (52 profiles, ~20M reads/sample; Supplementary Table 2) stimulated with IL15 (700 pM) and/or IL21 (20 pM) revealed that 4829 genes were differentially expressed (DEGs) compared to unstimulated cells in response to IL15, whereas IL21 induced only 601 DEGs (Figure 2A and Supplementary Table 3); 486 were shared genes, 115 and 4343 were differentially expressed selectively in response to IL21 (*IL21 specific*), and IL15 (*IL15 specific*), respectively. The evidence that IL15 can induce more massive transcriptional changes than IL21 prompted us to investigate whether and how IL21 altered IL15-driven transcriptional response in IE-CTL. The significance of the inquiry was further supported by the observation that IL15 is overexpressed in the intestinal epithelium of a subset of family members of patients with celiac disease, lacking any signs of adaptive anti-gluten immunity,¹¹ whereas IL21 is produced by gluten-specific T cells¹³ in the gut of active patients with villous atrophy. To address this question, we interrogated the RNA-seq data and identified 48 genes ($FDR < 0.05$) for which the intensity of the response to IL15 changed when IL21 was added (Figure 2B). Interestingly, most of these genes (35/48, 73%) were further upregulated on IL15+IL21 stimulation (group 4). The genes more strongly upregulated by IL15+IL21 vs IL15 alone (red in Figure 2C) contribute to immune pathways such as *defense response and regulation of cytokine production* and *cytokine-mediated signaling pathways*, as highlighted by the gene ontology enrichment analysis

(Figure 2D). Among these genes were granzyme B (*GZMB*), *STAT3*, *FOXO3*, *BATF*, *BCL3*, *MX1*, and *NOTCH1* (Figure 2B). Furthermore, 6 genes, including *RUNX2* and metabolic genes such as *VDR* were upregulated in response to IL15+IL21, despite being downregulated in response to IL15 alone (Figure 2B, group 3), suggesting that in few cases IL21 could reverse the effect of IL15.

Taken together, these observations suggest that, despite IL15 having a major impact on IE-CTL, IL21 has the capacity to further enhance IL15-driven transcriptional signature.

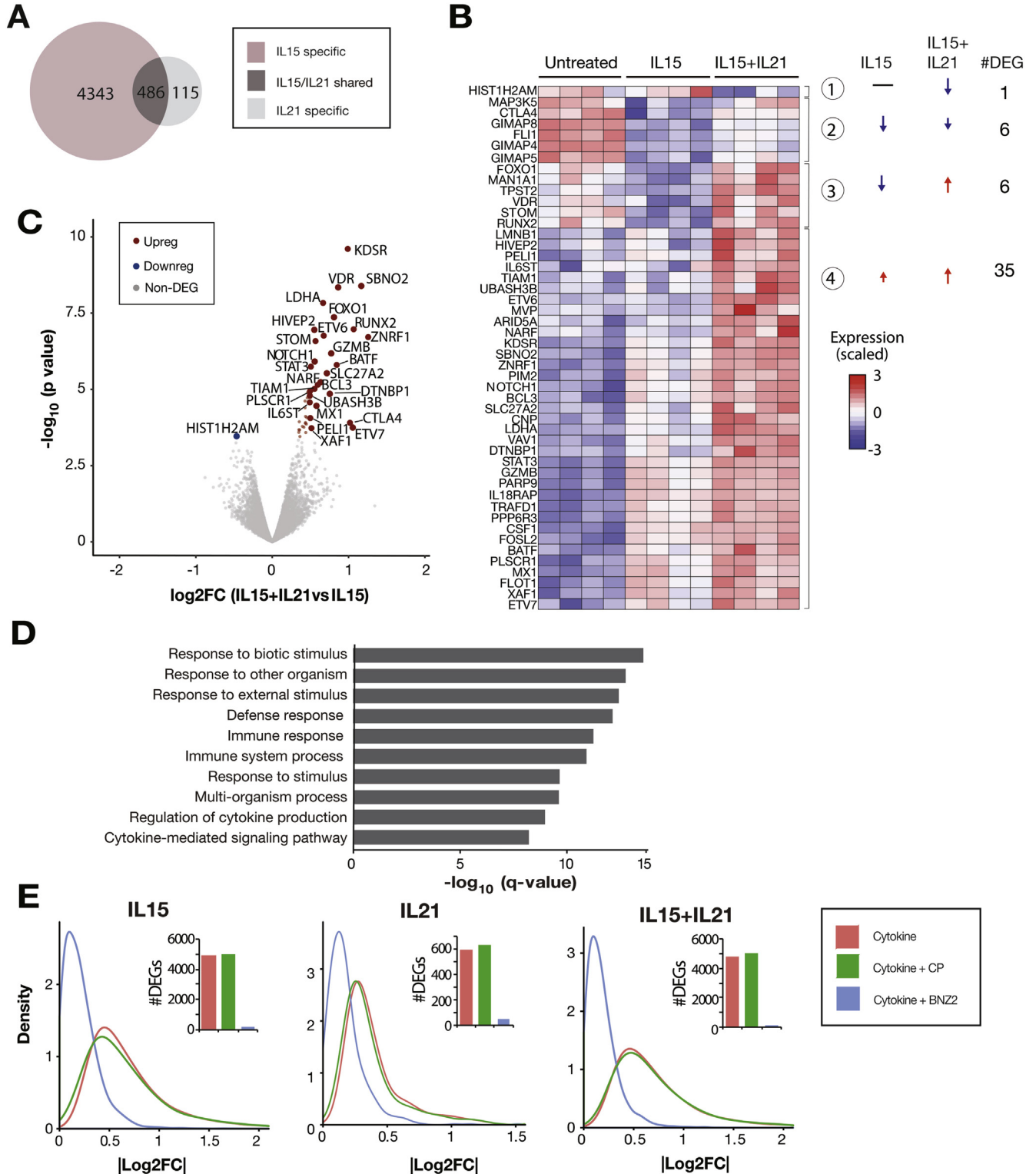
BNZ-2 Prevents IL15- and IL21-mediated Transcriptional Changes in IE-CTL Lines and in the Epithelial Compartment Ex Vivo

Next, we looked at the impact of BNZ-2 treatment on IL15- and/or IL21-driven transcriptional profile of IE-CTL. Importantly, BNZ-2, but not its scrambled sequence, reverted the transcriptional changes induced by IL15 and IL21 individually as well as combined (Figure 2E), attesting to its ability to prevent cytokine-mediated transcriptional reprogramming of IE-CTL lines.

Furthermore, we investigated whether BNZ-2 was effective under ex vivo conditions involving both epithelial cells and IE-CTL. Previous studies demonstrated that IL15 was not only expressed but also able to signal in intestinal epithelial cells.³⁴ The single-cell suspension obtained from the epithelial compartment of duodenal biopsies included approximately 80% of CD45⁺EpCam⁺ intestinal epithelial cells and 1% to 5% of CD45⁺EpCam⁻CD3⁺CD8⁺ IE-CTL as assessed by flow cytometry (Supplementary Figure 6A and B). Accordingly, when comparing transcriptional profiles of untreated IE-CTL lines and cells isolated ex vivo from the epithelial compartment to publicly available cell-type-specific data, ex vivo samples aligned with epithelial cell transcriptional profiles, whereas IE-CTL lines aligned with those from lymphocytes (Supplementary Figure 6C). Next, we assessed by RNA-seq the gene expression profile of the epithelial compartment upon stimulation with IL15 and/or IL21 for 2 hours. In addition, pSTAT3 and pSTAT5 were assessed by flow cytometry after 20 minutes (Supplementary Figures 6A and 7A and B). Ex vivo transcriptional data revealed 175 and 36 DEGs in response to IL15 and IL21, respectively, including 24 shared DEGs (Supplementary Figure 6D and Supplementary Table 3). Gene ontology analysis revealed a much stronger impact of IL15 on both immune- and nonimmune-related genes as compared with IL21 (Supplementary Figure 6E and Supplementary Table 4). Importantly, looking at the baseline expression levels in vitro vs ex vivo of the genes significantly changed in response to IL15 and/or IL21 ex vivo (Figure 3A), we identified a subset only expressed ex vivo (on the left side of the plot, Figure 3A), including mainly epithelial genes. In particular, genes coding for apolipoproteins (*APOA1* and 4), junctional proteins (*CLDN3*, 4, 23, and *PTPRF*) and epithelial transporters (*SLC6A19*, *PIGR*, *SLC39A5*) were selectively modulated by IL15, whereas the gene coding for the enzyme gastrin (*GAST*) was selectively changed by IL21 (Figure 3A). Nevertheless,

despite the presence of genes selectively changed ex vivo, a concordant response was observed between cell lines and ex vivo samples for IL15 ($r = 0.451$; $P = 2.254e^{-11}$) and IL21 ($r = 0.58$; $P = .000361$) responsive genes (Supplementary Figure 5F).

In accordance with our observations in IE-CTL lines (Figure 3B), a distinct ex vivo transcriptional profile emerged in response to combined IL15 and IL21 as compared with IL15 stimulation alone (Figure 3B). Of note, *GZMB* was the highest upregulated gene in the



ex vivo analysis. In addition, there was a significant upregulation of perforin (*PRF1*), suggesting that the 2 cytokines cooperatively enhance IE-CTL cytolytic program. Importantly, BNZ-2 efficiently prevented IL15/IL21-mediated transcriptional alterations not only in IE-CTL lines (Figure 2E), but also in the small intestinal epithelial compartment as a whole, including both IE-CTL and epithelial cells (Figure 3C). Finally, BNZ-2 blocked STAT5 and STAT3 phosphorylation upon IL15 (Supplementary Figure 7A and S8A) and IL21 (Supplementary Figure 7B) stimulation, respectively.

Together, these results indicate that IL15 and IL21 can reprogram IE-CTL and epithelial cells ex vivo. Furthermore, they demonstrate the ability of BNZ-2 to block the cytokine-induced reprogramming in a setting that reproduces, at least to a degree, the complexity of the small intestinal epithelial compartment where both lymphocytes and epithelial cells can respond to the presence of IL15 and IL21.

BNZ-2 Blocks IL15 and IL21-mediated Synergistic Activation of IE-CTL Ex Vivo

Having proven that IL21 could further modulate IL15-induced gene transcriptional profile in IE-CTL (Figure 1D and 2C), we analyzed the impact of the 2 cytokines on GzmB production (Figure 3D) and IE-CTL proliferation (Supplementary Figure 7C) by flow cytometry in freshly isolated IE-CTL from patients with celiac disease and controls. As anticipated, IL15 and IL21 synergistically increased the frequency of GzmB⁺ IE-CTL (Figure 3D). Moreover, their combination led to increased IE-CTL proliferation, as assessed by Ki67 staining (Supplementary Figure 7C). Importantly, BNZ-2, but not its scrambled sequence, reverted the functional synergistic effects of IL15 and IL21 on GzmB expression (Figure 3E and Supplementary Figure 8B) and IE-CTL proliferation (Supplementary Figure 7C).

Altogether, these results indicate that IL15 and IL21 may synergistically promote the expansion of IE-CTL and their ability to kill epithelial cells in active patients with celiac disease. Furthermore, the combined effect of IL15 and IL21 on IE-CTL can be blocked by BNZ-2.

BNZ-2 Prevents Cytokine and Gliadin-induced Release of IFN- γ

Gliadin, the dietary protein responsible for celiac disease development, was reported to increase the production of IL15,²¹ IL21,^{7,25} and IFN- γ ³⁵ in small intestinal biopsies of patients with celiac disease. Furthermore, IL15 in synergy with IL21 was proven to upregulate IFN- γ .³⁰ Importantly, BNZ-2 prevented the increase in IFN- γ transcript levels in IE-CTL in response to IL15 and IL21 stimulation alone or in combination (Supplementary Figure 9A).

Next, we determined whether BNZ-2 could prevent the release of IFN- γ in intestinal organ cultures in response to gliadin via its ability to block IL15- and IL21-mediated signaling. Duodenal organ culture generated from biopsies of patients with active celiac disease were stimulated with 1 mg/mL of peptic-tryptic digest of gliadin in presence or absence of BNZ-2. As displayed in Supplementary Figure 9B, IFN- γ produced in response to pepto-tryptic digest of gliadin stimulation in the supernatants of organ cultures ($P < .01$) was significantly reduced in presence of BNZ-2 ($P < .05$). These results further suggest that BNZ-2 may prevent the pathogenic effects of gluten challenge in patients with celiac disease.

BNZ-2 Specifically Blocks IL15, Without Impacting IL2-mediated Activation of IE-CTL

IL2, IL4, IL7, IL9, IL15, and IL21 all interact with the common γ c (IL2R γ) via the γ c box present in their D-helices.¹⁷ Each γ c box is composed of a unique sequence of amino acids. BNZ-2, similarly to BNZ-1, which selectively blocks IL2, IL9, and IL15, was designed based on the structural information of the γ c-cytokine binding site. More specifically, the sequence of BNZ-1 is a composite of the IL2 and IL15 D-helices, whereas BNZ-2 is a composite of IL15 and IL21. Importantly, BNZ-2 shares 13 and 15 residues with IL15 and IL21, respectively, and only 6 amino acids with IL2 (Figure 4A).

IL2 was indicated, in contrast to IL15, to prevent organ-specific autoimmunity.⁹ In addition to the γ c, it also shares the IL2R β signaling subunit with IL15.³⁶ To determine whether BNZ-2 would block IL15 while preserving IL2

Figure 2. BNZ-2 blocks the transcriptional program individually and cooperatively induced by IL15 and IL21 in tissue-resident IE-CTL. (A) Venn Diagram displaying the numbers of DEGs in response to 700 pM IL15 or 20 pM IL21. The expression of 4343 genes changed in response to IL15 (FDRIL15 <0.05 and FDRIL21 \geq 0.05, IL15 specific, pink), and 115 in response to IL21 (FDRIL15 \geq 0.05 and an FDRIL21 <0.05, IL21 specific, light gray); 486 genes are changed by both cytokines (FDRIL15 <0.05 and FDRIL21 <0.05, IL15/IL21 shared, dark gray). (B) Heat-map displaying changes in expression levels on stimulation with IL15 alone (FDRIL15 <0.05) or IL15+IL21 (FDRIL15 <0.05 and FDRIL21 <0.05) combination compared with untreated IE-CTL lines. Only DEGs in response to IL21+IL15 vs IL15 alone are displayed: 4 distinct groups were identified based on their change in expression levels. Arrows indicate up- vs downregulation. Numbers of DEGs in each group are indicated. (C) Volcano plot displaying DEGs in response to the combination of IL15+IL21 vs IL15. Expression levels after stimulation with IL15 were used as a baseline. P values are on the y-axis, log₂ fold changes (log₂FC) in expression on IL21 addition (IL15+IL21 vs IL15) are on the x-axis. The upregulated genes are in red on the right side, the only downregulated gene is in blue on the left. (D) Gene ontology (GO) enrichment analysis performed including all upregulated genes ($n = 41$) when IL21 is added to IL15 (red dots in B), ranked based on P values. Corrected P value (q-value) for enrichment of DEGs in each GO term is displayed. (E) Density plots representing the impact of 1 μ M BNZ-2 (blue) on IL15 and/or IL21-induced (red) differential gene expression in IE-CTL lines. A scrambled sequence of BNZ-2 served as control peptide (CP, green). Absolute log₂FC are on the x-axis. Number of DEGs is in the histograms. All data (A–E) are based on gene expression levels in human IE-CTL lines as assessed by RNA-seq. FDR <0.05 was used as a cutoff to evaluate DEGs.

signaling in IE-CTL lines, we analyzed induction of pSTAT5 (Figure 4B and C). Remarkably, BNZ-2 blocked IL15 (top) but not IL2 signaling (bottom), even when IL2 was used at low concentration (100 pM).

In line with the ability of BNZ-2 to block IL15 but not IL2 signaling, 1 μ M BNZ-2 impaired IL15-mediated (Figure 4D), but not IL2-mediated (Figure 4E), upregulation of *GZMB* transcripts ($P < .05$) (Supplementary Figure 5) and protein

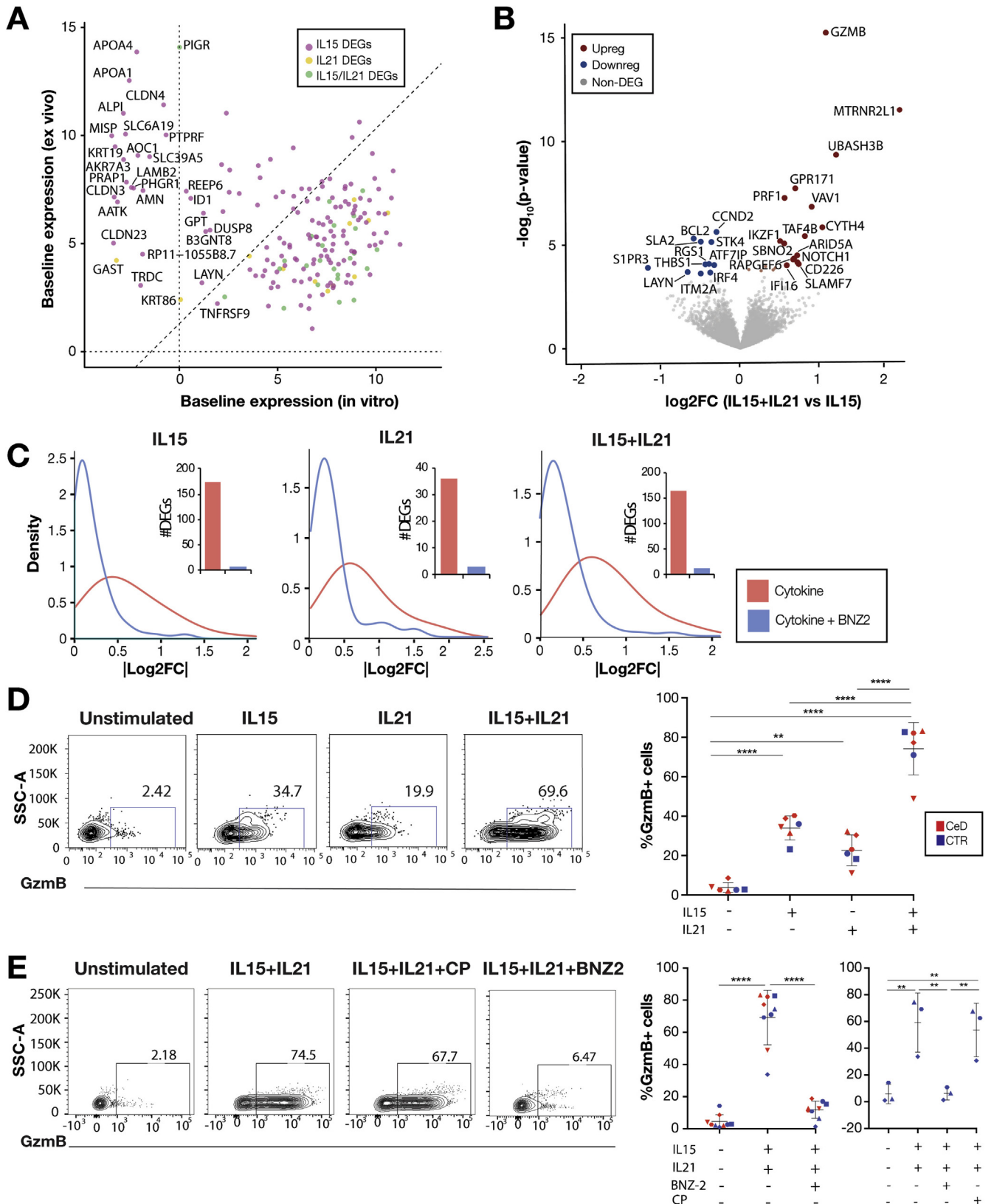


(Figure 4F) in IE-CTL lines, assessed by qPCR and flow cytometry, respectively. The EC₅₀, determined by qPCR for each cytokine (Supplementary Figure 5), was used for these experiments.

The extent to which BNZ-2 was able to block IL15 signaling depended also on the concentration of IL15 used to stimulate IE-CTL. More specifically, 3 μ M of BNZ-2 reduced pSTAT5 mean fluorescence intensity from 500 to 300, and from 400 to approximately 200 when 700 pM (high dose) and 100 pM (low dose) of IL15 was used, respectively (Figure 4C). In addition, the impact of higher doses of IL15 on the upregulation of *GZMB* transcript levels was dose-dependent (Supplementary Figure 10), indicating that it may be possible to calibrate the in vivo impact of BNZ-2 by adjusting its dose. In particular, to preserve the physiological functions of IL15 at low concentration, while preventing its pathogenic effects at high concentrations.

Because IL7, another member of the γ c cytokine family, plays an important role in survival and proliferation of human T cells,³⁷ and in intestinal homeostasis,³⁸ we determined the impact of BNZ-2 on IL7-mediated signaling in IE-CTL. Ex vivo analysis of pSTAT5 by flow cytometry proved that IL7-mediated increase in pSTAT5 was not impaired by BNZ-2 (Supplementary Figure 11A and B). Preservation of IL7 and IL2 signaling in the presence of BNZ-2 was further confirmed by WB in IE-CTL lines (Supplementary Figure 11C–E). Finally, because the γ c receptor is also shared with other γ c cytokines, we confirmed that BNZ-2 selectively prevented IL21- and IL15-mediated, but not IL2-, IL9-, or IL4-mediated, proliferation in NK92 cells (Supplementary Figure 12).

Together, these results indicate that BNZ-2 is an effective yet modifiable compound, that selectively inhibits IL15 and IL21 signaling. In particular, it preserves IL2 signaling (Figure 4 and Supplementary Figure 11), despite IL2 sharing the same signaling receptor as IL15.

Discussion

Our study reveals that celiac disease with villous atrophy, in contrast to potential celiac disease, is characterized by the concomitant overexpression of IL15 and IL21 in the

intestinal mucosa. Furthermore, our data indicate that IL15 and IL21 synergize in tissue-resident IE-CTL activation, and promote nonredundant signaling pathways. In particular, IL15 induced pSTAT5 and IL21 pSTAT3, whereas they cooperatively enhanced pSTAT1 and synergistically increased cytolytic properties and proliferation in IE-CTL. Altogether, these findings support a cooperative role for IL15 and IL21 in promoting tissue damage in celiac disease. Notably, we identify BNZ-2 as a novel γ c-binding peptide that concurrently inhibits IL15- and IL21-mediated activation of tissue-resident IE-CTL, while preserving IL2 signaling, suggesting that BNZ-2 represents a unique novel therapeutic candidate for active patients with celiac disease.

In addition to indicating that IL15 and IL21 induce distinct and non-overlapping signaling pathways, our study also provides support to the concept that IL21 may cooperate with IL15 to promote active celiac disease by enhancing IL15-driven transcriptional signature in human IE-CTL. Even though IL15 induces massive transcriptional changes in IE-CTL, IL21 enhances the impact of IL15 by upregulating genes associated with important immune functions (*RUNX2*, *FOXO1*, *BATF*, *STAT3*, *BCL3*, and *NOTCH1*). Ex vivo studies further confirmed that IL21 enhanced IL15-mediated transcriptional reprogramming of IE-CTL. In particular, IL15 in combination with IL21 led to a more significant upregulation of *GZMB*, *PRF1*, *VAV1*, and *NOTCH1* and downregulation of *RGS1* and *IRF4*, vs IL15 alone. Moreover, nonsaturating concentrations of the 2 cytokines synergistically promoted *GzmB* (Figure 3D) and IFN- γ (Supplementary Figure 9A) production and enhanced IE-CTL proliferation (Supplementary Figure 7C). Altogether, our ex vivo observations provide evidence that IL15 and IL21 cooperatively and non-redundantly activate human IE-CTL, key effector tissue-resident cell type mediating tissue destruction in celiac disease. Importantly, our finding that only patients with active, but not potential celiac disease had increased expression of both cytokines, further supports the concept that the 2 cytokines have a role in overt inflammation. In accordance, a recently published clinical trial³⁹ reports that anti-IL15 monoclonal antibody failed to prevent mucosal injury in response to gluten challenge, despite reducing CD3⁺

Figure 3. Cooperative and synergistic effects of IL15 and IL21 in the small intestinal epithelial compartment are efficiently blocked by BNZ-2 ex vivo. (A) Scattered plot displaying DEGs in response to IL15 only (FDRIL15 <0.05 and FDRIL21 \geq 0.05, purple dots), IL21 only (FDRIL21 <0.05 and FDRIL15 \geq 0.05, yellow dots) or their combination (FDRIL15 <0.05 and FDRIL21 <0.05, green dots) ex vivo. Baseline expression levels ex vivo (y) and in vitro in cell lines (x) are plotted for each gene. Correlation between ex vivo and in vitro expression: $r = -0.33$, Pearson's test. (B) Volcano-plot displaying genes significantly changed in response to IL15+IL21 vs IL15 only (baseline), P values are plotted on the y-axis, log₂FC in expression when adding IL21 (IL15+IL21 vs IL15) on the x-axis. Upregulated genes are in red, the downregulated are in blue. (C) Density plots indicating the impact of BNZ-2 (blue) on IL15- and IL21-induced (red) gene expression changes. Number of DEGs is indicated in the histograms in each plot. Data in (A–C) were assessed by RNA-seq in a single-cell suspension of the epithelial compartment stimulated ex vivo with 700 pM of IL15 and/or 20 pM of IL21, in presence or absence of 1 μ M BNZ-2. FDR <0.05 was used to evaluate DEGs. (D, E) On the left, representative FACS plot displaying *GzmB* intracellular expression in live CD3⁺CD8⁺ cells in response to IL15 (700 pM), IL21 (20 pM), and their combination (D), and the impact of 1 μ M of BNZ-2 or a control peptide (CP, E). On the right, quantification of 6 experiments (D), including 4 GFD patients (red) and 2 Controls (CTR, blue) and of 9 experiments (E, left plot), including 4 GFD patients (red) and 5 CTR, (blue) with BNZ-2 and 3 experiments in CTR with the CP (E, right plot). A single-cell suspension of the duodenal epithelial compartment was stained ex vivo and analyzed by flow cytometry. Each distinct symbol shape refers to an individual. Paired 1-way analysis of variance was performed, ** $P < .01$, *** $P < .001$, **** $P < .0001$.

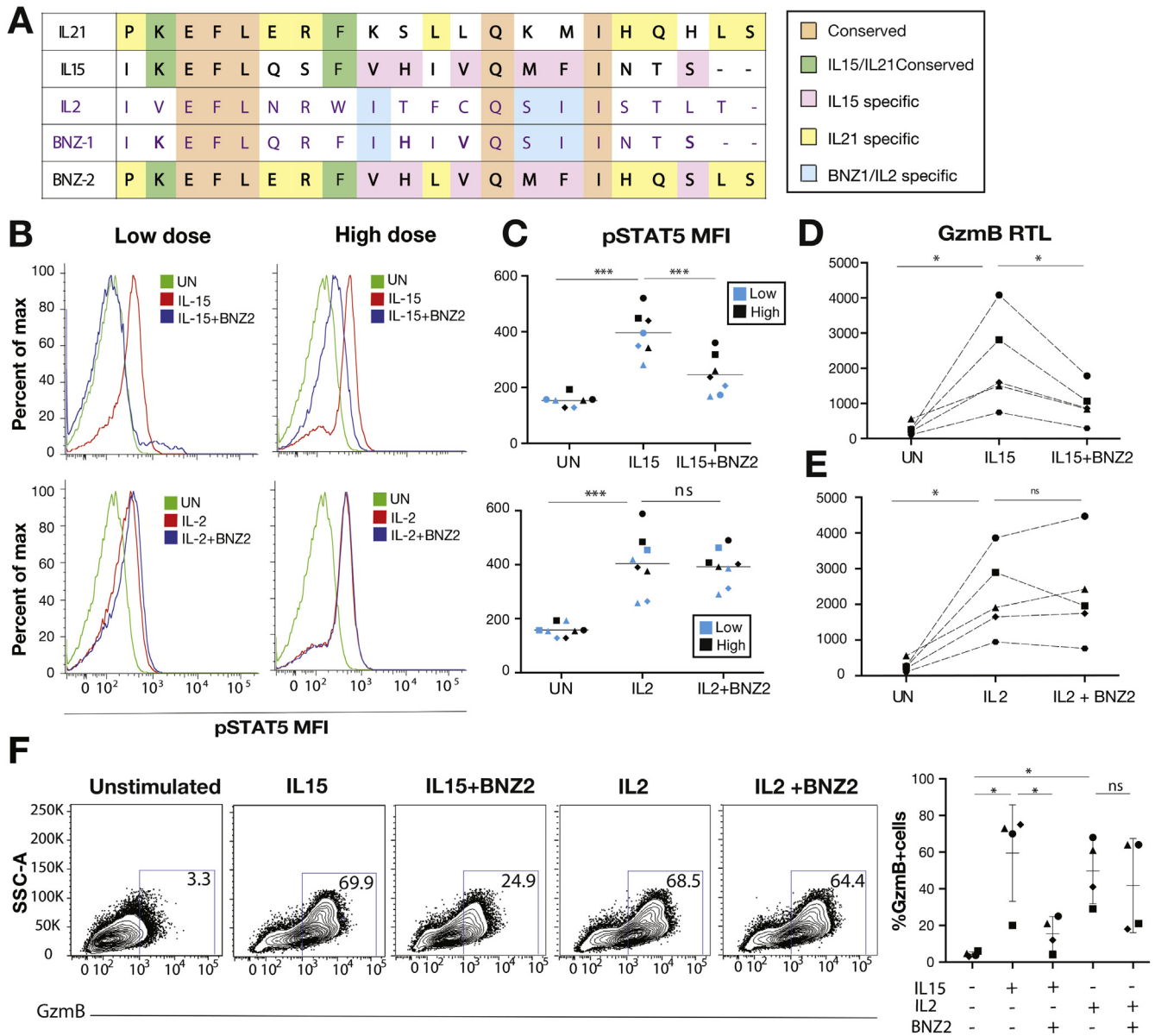


Figure 4. BNZ-2 specifically inhibits IL15 but not IL2-mediated changes in signaling and function in tissue-resident IE-CTL. (A) Alignment of BNZ-1 and -2 with IL2, IL21, and IL15. The aminoacidic sequences of the D-helices for the 3 γ c cytokines: IL2 (purple font), IL15, and IL21 (black font) were aligned to those of BNZ-1 (purple font) and BNZ-2 (black font). Shared residues are highlighted in a color-coded fashion: in common to all cytokines and both BNZ-1 and BNZ-2 (orange), conserved between IL21, IL15, and BNZ-2 (green), shared by BNZ-2 only with IL15 (pink) and IL21 (yellow), in common to BNZ-1 and IL2 (light blue). (B) Representative density plot displaying the mean fluorescence intensity of pSTAT5 in response to 100 pM (left) and 700 pM (right) of IL15 (top) or IL2 (bottom) with or without 3 μ M BNZ-2 (blue) in IE-CTL lines, as compared with unstimulated (UN) cells (green). Mean fluorescence intensity quantification in response to low (blue) and high (black) concentrations of IL15 and IL2. (C) pSTAT5 MFI. (D, E) GzmB relative transcripts levels (RTL) in response to IL15 (D) or IL2 (E) with or without 1 μ M BNZ-2. (F) Intracellular expression of GzmB in response to IL15 or IL2 with or without 1 μ M BNZ-2. One representative plot (left) and frequency of GzmB⁺ cells in 4 independent experiments (right). (A–F) paired 1-way analysis of variance, **P* < .05, ****P* < .001. (C–F) Each symbol refers to a distinct cell line.

epithelial infiltration in patients with celiac disease. This indicates that blocking IL15 alone is not sufficient, and that targeting IL21 in addition may contribute to prevent villous atrophy.

In recent years, a strategy based on the usage of peptides that share specific amino acids with particular γ c cytokines was designed to target the binding interface on the γ c

receptor and selectively block their signaling, without impairing other γ c cytokines.¹⁷ This is of particular interest for diseases in which multiple cytokines of the same family are involved. The first multi- γ c-cytokines inhibitor, BNZ-1, was designed to block IL2, IL9, and IL15^{17–18} and proved to decrease regulatory T cells, natural killer (NK) cells, and CD8⁺ Central Memory T-Cells in T-Cell malignancies.¹⁹

Thanks to its safety profile, it is currently tested in phase I clinical trials for T-cell large granular lymphocyte leukemia, and refractory cutaneous T-cell lymphoma ([ClinicalTrials.gov Identifier: NCT03239392](https://clinicaltrials.gov/Identifier/NCT03239392)). BNZ-2, a novel peptide with a distinct amino acidic sequence, inhibits individual and cooperative effects of IL15 and IL21 in human IE-CTLs without interfering with other γ c cytokines, in particular IL2. This is remarkable given that IL2 and IL15 share the same heterodimeric signaling receptor (IL2/IL15R $\beta\gamma$). The rationale behind wanting to preserve IL2 signaling lies in its key function in immune tolerance through its role in regulatory forkhead box P3 (Foxp3⁺) T-cell homeostasis.¹⁰

In addition to being a potential treatment for patients with active celiac disease, BNZ-2 may represent an approach to prevent development of RCD. Although several studies pointed to a critical role for IL15 in the pathogenesis of RCD, 3 distinct sets of evidence indicate that blocking IL21 in addition to IL15 may contribute to prevent future RCD development in patients with celiac disease: (1) RCD onset is linked to the intensity of the anti-gluten CD4⁺ T-cell response associated with IFN- γ and IL21 production,⁴⁰ indeed HLA-DQ2 homozygous subjects are at higher risk for RCD⁴¹; (2) IL21 promotes pSTAT3 and IEL cytolytic function ([Figure 2D](#)); (3) mutations facilitating IL15 mediated STAT3 activation are positively selected in refractory IELs.^{16,42} Despite potentially useful to prevent its development, a strategy blocking also IL21 would have no additional advantage over anti-IL15 treatment for established RCD on a GFD because STAT3 activation can be induced by IL15 alone and does not depend on IL21 in IELs.⁴³ Moreover, IE-CTL cytolytic properties and consequently villous atrophy, persists even on a GFD, indicating that IFN- γ and IL21 produced by gluten-specific CD4⁺ T cells¹² are not critical in RCD. Taken together, these observations indicate that BNZ-2 might be effective in preventing, but not treating, RCD ([Supplementary Figure 13](#)).

In summary, our study suggests that BNZ-2 is a unique therapeutic candidate for active celiac disease where IL15 and IL21 play a joint role in the activation of tissue-resident IE-CTL that mediate tissue destruction and can undergo STAT3-dependent lymphomagenesis.^{40,42} Importantly, BNZ-2 will be effective in more than 70% of patients with celiac disease, targeting not only those overexpressing IL15 or IL21, but also 57% of patients upregulating both. Furthermore, suggesting that PEGylated BNZ-2 will be effective in patients, BNZ-1 has been proven to have a good pharmacodynamic profile in vivo in humans in its PEGylated form.¹⁹ This novel approach has the dual advantage of being more wide-ranging than targeting a single cytokine (ie, anti-IL15 blockers^{43,44}) and more specific than blocking a wide range of cytokines (ie, JAK inhibitors⁴⁵).

More generally, BNZ-2 also may have a therapeutic potential in other autoimmune disorders, such as type 1 diabetes^{2,3} and graft-versus-host disease,^{4,5} in which IL15- and IL21-driven activation of CTL plays a critical role in tissue destruction. Finally, whether BNZ-2 might exert wider effects, including blocking IL21-mediated B-cell activation and antibody production, remains to be demonstrated.

Supplementary Material

Note: To access the supplementary material accompanying this article, visit the online version of *Gastroenterology* at www.gastrojournal.org, and at <https://doi.org/10.1053/j.gastro.2019.10.006>.

References

1. Rochman Y, Spolski R, Leonard WJ. New insights into the regulation of T cells by gamma(c) family cytokines. *Nat Rev Immunol* 2009;9:480–490.
2. Spolski R, Kashyap M, Robinson C, et al. IL-21 signaling is critical for the development of type I diabetes in the NOD mouse. *Proc Natl Acad Sci U S A* 2008;105:14028–14033.
3. Chen J, Feigenbaum L, Awasthi P, et al. Insulin-dependent diabetes induced by pancreatic beta cell expression of IL-15 and IL-15Ralpha. *Proc Natl Acad Sci U S A* 2013;110:13534–13539.
4. Blaser BW, Roychowdhury S, Kim DJ, et al. Donor-derived IL-15 is critical for acute allogeneic graft-versus-host disease. *Blood* 2005;105:894–901.
5. Hippen KL, Bucher C, Schirm DK, et al. Blocking IL-21 signaling ameliorates xenogeneic GVHD induced by human lymphocytes. *Blood* 2012;119:619–628.
6. Jabri B, Abadie V. IL-15 functions as a danger signal to regulate tissue-resident T cells and tissue destruction. *Nat Rev Immunol* 2015;15:771–783.
7. Fina D, Sarra M, Caruso R, et al. Interleukin 21 contributes to the mucosal T helper cell type 1 response in celiac disease. *Gut* 2008;57:887–892.
8. Ross SH, Cantrell DA. Signaling and function of interleukin-2 in T lymphocytes. *Ann Rev Immunol* 2018;36:411–433.
9. Waldmann TA. The biology of interleukin-2 and interleukin-15: implications for cancer therapy and vaccine design. *Nat Rev Immunol* 2006;6:595–601.
10. Josefowicz SZ, Lu LF, Rudensky AY. Regulatory T cells: mechanisms of differentiation and function. *Annu Rev Immunol* 2012;30:531–564.
11. Setty M, Discepolo V, Abadie V, et al. Distinct and synergistic contributions of epithelial stress and adaptive immunity to functions of intraepithelial killer cells and active celiac disease. *Gastroenterology* 2015;149:681–691.e610.
12. Bodd M, Ráki M, Tollefsen S, et al. HLA-DQ2-restricted gluten-reactive T cells produce IL-21 but not IL-17 or IL-22. *Mucosal Immunol* 2010;3:594–601.
13. Borrelli M, Gianfrani C, Lania G, et al. In the intestinal mucosa of children with potential celiac disease IL-21 and IL-17A are less expressed than in the active disease. *Am J Gastroenterol* 2016;111:134–144.
14. Zeng R, Spolski R, Finkelstein SSE, et al. Synergy of IL-21 and IL-15 in regulating CD8⁺ T cell expansion and function. *J Exp Med* 2005;201:139–148.
15. Rubio-Tapia A, Hill ID, Kelly CP, et al. American College of Gastroenterology. ACG clinical guidelines: diagnosis and management of celiac disease. *Am J Gastroenterol* 2013;108:656–676.

16. Malamut G, Cellier C. Refractory celiac disease. *Gastroenterol Clin North Am* 2019;48:137–144.
17. Nata T, Basheer A, Cocchi F, et al. Targeting the binding interface on a shared receptor subunit of a cytokine family enables the inhibition of multiple member cytokines with selectable target spectrum. *J Biol Chem* 2015;290:22338–22351.
18. Massoud R, Enose-Akahata Y, Tagaya Y, et al. Common gamma-chain blocking peptide reduces in vitro immune activation markers in HTLV-1-associated myelopathy/tropical spastic paraparesis. *Proc Natl Acad Sci U S A* 2015;112:11030–11035.
19. Frohna P, Tagaya Y, Ratnayake A, et al. Results from a first-in-human study with Bnz-1: a novel peptide inhibitor of IL-2, IL-9 and IL-15 for the treatment of T-cell malignancies that safely and selectively decreases regulatory T-Cells, natural killer cells, and CD8+ central memory T-cells. *Blood* 2017;130:695.
20. Husby S, Koletzko S, Korponay-Szabó IR, et al. European Society for Pediatric Gastroenterology, Hepatology, and Nutrition guidelines for the diagnosis of coeliac disease. *J Pediatr Gastroenterol Nutr* 2012;54:136–160.
21. Maiuri L, Ciacci C, Auricchio S, et al. Interleukin 15 mediates epithelial changes in celiac disease. *Gastroenterology* 2000;119:996–1006.
22. Mention JJ, Ben Ahmed M, Bègue B, et al. Interleukin 15: a key to disrupted intraepithelial lymphocyte homeostasis and lymphomagenesis in celiac disease. *Gastroenterology* 2003;125:730–745.
23. Sarra M, Cupi ML, Monteleone I, et al. IL-15 positively regulates IL-21 production in celiac disease mucosa. *Mucosal Immunol* 2013;6:244–255.
24. Fehniger TA, Caligiuri MA. Interleukin 15: biology and relevance to human disease. *Blood* 2001;97:14–32.
25. Jabri B, Sollid LM. Tissue-mediated control of immunopathology in celiac disease. *Nat Rev Immunol* 2009;9:858–870.
26. Abadie V, Discepolo V, Jabri B. Intraepithelial lymphocytes in celiac disease immunopathology. *Semin Immunopathol* 2012;34:551–566.
27. Johnston JA, Bacon CM, Finbloom DS, et al. Tyrosine phosphorylation and activation of STAT5, STAT3, and Janus kinases by interleukins 2 and 15. *Proc Natl Acad Sci U S A* 1995;92:8705–8709.
28. Lin JX, Migone TS, Tseng M, et al. The role of shared receptor motifs and common Stat proteins in the generation of cytokine pleiotropy and redundancy by IL-2, IL-4, IL-7, IL-13, and IL-15. *Immunity* 1995;2:331–339.
29. Miyazaki T, Kawahara A, Fujii H, et al. Functional activation of Jak1 and Jak3 by selective association with IL-2 receptor subunits. *Science* 1994;266:1045–1047.
30. Strengell M, Matikainen S, Sirén J, et al. IL-21 in synergy with IL-15 or IL-18 enhances IFN-gamma production in human NK and T cells. *J Immunol* 2003;170:5464–5469.
31. Marzec M, Halasa K, Kasprzycka M, et al. Differential effects of interleukin-2 and interleukin-15 versus interleukin-21 on CD4+ cutaneous T-cell lymphoma cells. *Cancer Res* 2008;68:1083–1091.
32. Spolski R, Leonard WJ. Interleukin-21: basic biology and implications for cancer and autoimmunity. *Annu Rev Immunol* 2008;26:57–79.
33. Pouw N, Treffers-Westerlaken E, Kraan J, et al. Combination of IL-21 and IL-15 enhances tumour-specific cytotoxicity and cytokine production of TCR-transduced primary T cells. *Cancer Immunol Immunother* 2010;59:921–931.
34. Reinecker HC, MacDermott RP, Mirau S, et al. Intestinal epithelial cells both express and respond to interleukin 15. *Gastroenterology* 1996;111:1706–1713.
35. Nilsen EM, Jahnsen FL, Lundin KE, et al. Gluten induces an intestinal cytokine response strongly dominated by interferon gamma in patients with celiac disease. *Gastroenterology* 1998;115:551–563.
36. Ring AM, Lin JX, Feng D, et al. Mechanistic and structural insight into the functional dichotomy between IL-2 and IL-15. *Nat Immunol* 2012;13:1187–1195.
37. Niu N, Qin X. New insights into IL-7 signaling pathways during early and late T cell development. *Cell Mol Immunol* 2013;10:187–189.
38. Belarif L, Danger R, Kermarrec L, et al. IL-7 receptor influences anti-TNF responsiveness and T cell gut homing in inflammatory bowel disease. *J Clin Invest* 2019;129:1910–1925.
39. Lähdeaho ML, Scheinin M, Vuotikka P, et al. Safety and efficacy of AMG 714 in adults with coeliac disease exposed to gluten challenge: a phase 2a, randomised, double-blind, placebo-controlled study. *Lancet Gastroenterol Hepatol* 2019;4:948–959.
40. Kooy-Winkelaar YM, Bouwer D, Janssen GM, et al. CD4 T-cell cytokines synergize to induce proliferation of malignant and nonmalignant innate intraepithelial lymphocytes. *Proc Natl Acad Sci U S A* 2017;114:E980–E989.
41. Al-Toma A, Goerres MS, Meijer JW, et al. Human leukocyte antigen-DQ2 homozygosity and the development of refractory celiac disease and enteropathy associated T-cell lymphoma. *Clin Gastroenterol Hepatol* 2006;4:315–319.
42. Ettersperger J, Montcuquet N, Malamut G, et al. Interleukin-15-dependent T-cell-like innate intraepithelial lymphocytes develop in the intestine and transform into lymphomas in celiac disease. *Immunity* 2016;45:610–625.
43. Morris JC, Janik JE, White JD, et al. Preclinical and phase I clinical trial of blockade of IL-15 using Mikbeta1 monoclonal antibody in T cell large granular lymphocyte leukemia. *Proc Natl Acad Sci U S A* 2006;103:401–406.
44. Yokoyama S, Watanabe N, Sato N, et al. Antibody-mediated blockade of IL-15 reverses the autoimmune intestinal damage in transgenic mice that overexpress IL-15 in enterocytes. *Proc Natl Acad Sci U S A* 2009;106:15849–15854.
45. Yokoyama S, Perera PY, Waldmann TA, et al. Tofacitinib, a janus kinase inhibitor demonstrates efficacy in an IL-15 transgenic mouse model that recapitulates pathologic manifestations of celiac disease. *J Clin Immunol* 2013;33:586–594.

Received May 16, 2019. Accepted October 4, 2019.

Correspondence

Address correspondence to: Bana Jabri, MD, PhD, Department of Medicine, University of Chicago, 900 East 57th Street, KCBD 9124, MB#9, Illinois 60637. e-mail: bjabri@bsd.uchicago.edu.

Acknowledgments

The authors thank all patients and their family members as well as the University of Chicago Celiac Disease Center for supporting our research. The authors thank Valerie Abadie, University of Chicago, for critical reading of the manuscript and fruitful discussion. The authors thank Vania Yotova and Anne Dumaine (CHU Sainte-Justine Research Center, Montreal, QC, Canada), Maria Vittoria Barone, and Giuliana Lania (University of Naples Federico II) for technical support. The authors thank Nicholas Di Nardi for helping consenting patients. Human recombinant IL2 used for stimulation of cell lines and ex vivo samples was obtained through the National Institutes of Health (NIH) AIDS Reagent Program, Division of AIDS, National Institute of Allergy and Infectious Diseases, NIH.

RNA-sequencing was performed by the University of Chicago Genomics Facility (<http://genomics.bsd.uchicago.edu>). The RNA-sequencing data reported in this paper were deposited into the National Center for Biotechnology Information Gene Expression Omnibus database under the SuperSeries record GSE120904.

Alain Pacis's current affiliation is: Canadian Centre for Computational Genomics, McGill University and Genome Quebec Innovation Center, Montreal, Quebec, Canada.

Author contributions: C.C. and V.D. performed and analyzed the experiments; V.D. and B.J. wrote the manuscript; A.P. and O.T. analyzed the transcriptional data; N.D. performed the WB; T.M. generated cell lines and contributed to the interpretation of the results; M.M. performed the organ culture experiments; A.B. and L.A.M. performed the proliferation and transcription assays to characterize BNZ-2; P.G. enrolled the patients from Columbia University; R.A. and R.T. enrolled the patients from the University of Naples; N.A. and Y.T. are responsible for the design and synthesis of BNZ-2; T.A.W. provided conceptual contributions; L.B.B. overviewed the computational analysis of the transcriptional data and contributed to the interpretation of the results; B.J. is responsible for the study concept and design and supervised the research.

Conflicts of interest

These authors disclose the following: Nick Doerr, Asjad Basheer, Laith Q. Al-Mawsawi, and Nazii Azimi are employees of BIONIZ therapeutics, the developer of the peptide used in this study. Bana Jabri is an advisor to and shareholder of BIONIZ therapeutics. BIONIZ therapeutics holds the US patent for the peptide. We also declare that the financial involvements of BIONIZ therapeutics did not undermine the scientific objectivity and integrity of the presented work. The remaining authors disclose no conflicts.

Funding

This work was supported by National Institutes of Health grant R01DK067180 to Bana Jabri. Additional support includes Cancer Center Support grant P30CA014599, Digestive Diseases Research Core Center P30 DK42086 at the University of Chicago to Bana Jabri and the "Carlino fellowship for celiac disease research" from the University of Chicago Celiac Disease Center to Valentina Discepolo. This work was also supported in part by research funding from BIONIZ therapeutics.

Supplementary Materials and Methods

Study Design

The overall hypothesis advanced by this study is that IL15 and IL21 synergize to drive cytolytic potential of human IE-CTL and that BNZ-2, by simultaneously blocking their combined effects, might represent a new therapeutic candidate for celiac disease and other immune disorders in which IL15 and IL21 mediate CTL activation. Celiac disease is the prototype of immune-mediated disorders in which IE-CTLs play a key role in tissue destruction, thus we designed a preclinical controlled laboratory study to dissect the impact of IL15 and IL21 on signaling, transcriptional program, and function of human IE-CTL and tested the blocking ability of BNZ-2. Two distinct experimental systems have been set up: (1) *in vitro*, using human short-term intraepithelial CD8⁺ T cell lines, and (2) *ex vivo*, using a single-cell suspension from the small intestinal epithelial compartment isolated from human duodenal biopsies. In each experimental system, we tested the individual and combined impact of IL15 and IL21 on (1) phosphorylation of signaling molecules by WB or phospho-flow cytometry, (2) gene transcriptional profile by RNA-seq, and (3) functional properties, looking at proliferation by Ki67 staining and granzyme (Gzm) B production by flow cytometry and IFN- γ by PCR. The ability of BNZ-2 to prevent cytokine-mediated effects was tested in both experimental systems, and a control peptide was included to ensure specificity. Because IL2 shares IL2/IL15R $\beta\gamma$ with IL15, the ability of BNZ-2 to impair IL15-, but not IL2-mediated effects on signaling, transcription, and cytolytic function, was also tested. Its ability to prevent other γ cytokine signaling was also investigated.

To support the translational relevance of the combined blockade of IL15 and IL21 in celiac disease, we looked at the expression of 2 cytokines in the small intestinal biopsies of patients with active and potential celiac disease. To ensure statistical power and reproducibility, in addition to technical replicates in each experiment, we performed a minimum of 3 biological replicates for signaling experiments, and a minimum of 5 biological replicates for RNA-seq. All samples were de-identified before running the experiments to guarantee a blind approach.

RNA Isolation From Small Intestinal Biopsies

To isolate RNA from whole duodenal biopsies, a single bioptic fragment was stored in RNA-later (QIAGEN, Hilden, Germany) at the time of endoscopy, kept at 4°C for 24 hours, and then frozen at -80°C on RNA-later removal until processing. Defrost tissues were homogenized using magnetic beads and a Cell Tissue Homogenizer (Bullet blender by Next Advance, Troy, NY) and RNA was extracted using RNeasy columns (QIAGEN). RNA integrity was assessed by Bioanalyzer (Agilent, Santa Clara, CA).

Taqman PCR

An amount of 500 ng of high-quality RNA was reverse-transcribed into complementary DNA (cDNA) using the

qScript cDNA SuperMix (Quanta Biosciences, Salt Lake City, UT). TaqMan Gene Expression Assay (Applied Biosystems [Foster City, CA], final concentration 1X) using Taqman Fast Advanced Master Mix and Taqman specific probes were used to measure the expression levels of *IL15Ra* (Hs00542604) and *IL21* (Hs00222327) genes. As house-keeping genes, we used: *GAPDH* (Hs02758991), *GUSB* (Hs99999908), *HPRT1* (Hs99999909), and *POLR2A* (Hs00172187). PCR was performed using the following thermal protocol: 50°C, 2 minutes; 95°C, 2 minutes, PCR Cycle of 40 cycles of (95°C, 1 second; 60°C, 20 seconds).

Intestinal Epithelial Compartment Isolation and Short-Term Intraepithelial CD8⁺ T-Cell Line Generation

Epithelial compartment was isolated from human duodenal biopsies via mechanical disruption. Briefly, 4 to 6 biopsies from each subject were collected in cell culture medium and suspended in 7 mL of 1640 RPMI containing 1% dialyzed fetal bovine serum (Biowest, Riverside, MO), 2 mM EDTA (Corning, Corning, NY), and 1.5 mM MgCl₂ (Thermo Fisher Scientific, Waltham, MA) and shaken at 250 rpm for 30 minutes at 37°C. The procedure was repeated twice with fresh medium to enhance cell recovery. Cells were harvested from biopsy-free media via centrifugation and pooled for subsequent use. Single-cell suspensions were used for *ex vivo* experiments. To generate short-term CD8⁺ lines, epithelial single-cell suspensions were stained with fluorochrome-labeled anti-human CD45 (BD Biosciences, San Jose, CA), CD3 (Biolegend, San Diego, CA), TCR $\alpha\beta$ (Biolegend), and CD8 α (BD Biosciences) antibodies and CD45⁺CD3⁺CD8⁺TCR $\alpha\beta$ ⁺-positive cells were purified via fluorescence activated cell sorting (FACS). Sorted CD8⁺ T cells were subsequently expanded *in vitro* with 1 μ g/mL phytohaemagglutinin (PHA; Calbiochem, San Diego, CA) and a mixture of irradiated heterologous peripheral blood leukocytes and Epstein-Barr virus-transformed cell lines in 1640 RPMI with 10% human serum AB (Atlanta Biologicals, Flowery Branch, GA) and maintained in culture for 10 to 12 days with 100 U/mL of IL2 (National Institutes of Health AIDS Reagent Program). Before IL15 and IL21 stimulation, cells were deprived of IL2 for 24 (before WB or phospho-flow cytometry) or 48 (before RNA-seq) hours and plated at a concentration of 1 \times 10⁶ cells/mL for stimulation and downstream experiments. No differences in survival, cytolytic properties, or response to cytokines were observed between cell lines generated from controls or patients with celiac disease.

Western Blotting

On indicated treatments, CD8⁺ T cells were collected, washed in PBS, and lysed in 200 μ L of NP-40 lysis buffer (NaCl 15 mM, 1% Triton X-100, 50 mM Tris at pH 8.0) supplemented with protease and phosphatase inhibitors (Fisher, Hampton, NH). Proteins were extracted and separated by sodium dodecyl sulfate-polyacrylamide gel electrophoresis using 4% to 12% gradient polyacrylamide gels (Novex, Life Technologies, Carlsbad, CA), transferred onto

polyvinylidene fluoride membrane (Novex, Life Technologies), blocked overnight with 5% nonfat dry milk in Tris-buffered saline containing 0.1% Tween-20 (TBST) buffer and immunoblotted with antibodies sourced from Cell Signaling Technologies (Danvers, MA) against pSTAT1 (catalog no. 9167, 1:3000 dilution), pSTAT3 (catalog no. 9145, 1:2000 dilution), pSTAT5 (catalog no. 9359, 1:4000 dilution), pAKT (catalog no. 4060, 1:2000 dilution), pERK1/2 (catalog no. 4370, 1:1500 dilution), ERK1/2 (catalog no. 4695, 1:2000 dilution), and β -actin (catalog no. 3700, 1:10,000 dilution). Bands were detected using a Li-Cor C-digit blot scanner and quantified with the associated Image Studio software (Li-Cor, Lincoln, NE).

qPCR

RNA (200 ng) was reverse-transcribed using the GoScript kit (Promega, Madison, WI). Gene expression levels were determined by SybrGreen-based qPCR using the following primers:

hGZMB-forward: 5'-CCCTGGGAAAACACTCACACA-3'
 hGZMB-reverse: 5'-GCACAACCTCAATGGTACTGTGCG-3'
 hSTAT3-forward: 5'-ACCAGCAGTATAGCCGCTTC-3'
 hSTAT3-reverse: 5'-GCCACAATCCGGGCAATCT-3'
 hTNFSF10-forward: 5'-TGCGTGCTGATCGTGATCTTC-3'
 hTNFSF10-reverse: 5'-GCTCGTTGGTAAAGTACACGTA-3'
 hIFNG-forward: 5'-TCGGTAACTGACTTGAATGTCCA-3'
 hIFNG-reverse: 5'-TCGCTTCCCTGTTTTAGCTGC-3'
 hGAPDH-forward: 5'-ATGGGGAAGGTGAAGTTCG-3'
 hGAPDH-reverse: 5'-GGGTCATTGATGGCAACAATA-3'

Ct values were obtained on LC480 qPCR System (Roche, Basel, Switzerland) and relative expression was calculated using the formula $2^{-\Delta Ct}$, where $\Delta Ct = Ct\text{-target gene} - Ct\text{-housekeeping gene GAPDH}$

Bulk RNA-sequencing Analysis of In Vitro and Ex Vivo Samples

Library Preparation and Sequencing. Cells were collected and homogenized in RLT plus buffer. RNA was isolated using the RNeasy Plus Mini Kit and RNeasy Plus Micro Kit (Qiagen) for cell lines and ex vivo samples, respectively, according to the manufacturer's instructions. RNA-seq libraries were prepared using the SMARTer Stranded Total RNA Sample Prep Kit-HI Mammalian by Clontech Laboratories (Takara, Kusatsu, Japan) for cell lines and the Illumina (San Diego, CA) TruSeq Total RNA stranded kit for ex vivo samples. Quality of both RNA (RIN >8) and libraries was assessed by Bioanalyzer (Agilent Technologies). Indexed cDNA libraries were pooled in equimolar amounts and sequenced with single-end 50-base pair reads with a high-output Flow Cell (8-lane flow cell) on an Illumina HiSeq4000 at the University of Chicago Genomic Facility. In vitro and ex vivo samples were run separately. Number of reads sequenced per sample are in [Supplementary Table 2](#).

RNA-seq Data Pre-processing. A total of $n = 52$ bulk RNA-seq samples from cell lines and $n = 35$ samples from ex vivo biopsies were processed in this study. Adaptor sequences and low-quality score bases were first trimmed

using Trim Galore (https://www.bioinformatics.babraham.ac.uk/projects/trim_galore/) with the following parameter: `-clip_R1 5`. The resulting reads were then mapped to the human genome reference sequence (GRCh37/hg19) using the TopHat2 software package¹ with a TopHat transcript index from Ensembl (Cambridge, United Kingdom). The number of reads overlapping with annotated exons of genes was tabulated using HTSeq² with the following parameters: `-q -m intersection-nonempty -s no`. For all downstream analyses, we excluded noncoding and lowly expressed genes with a median read count lower than 20 in all samples. This yielded $n = 10,694$ genes in the cell lines dataset, and $n = 11,740$ genes in the ex vivo dataset.

Identification of Differentially Expressed Genes Between Experimental Conditions

Gene expression levels across samples were normalized using the TMM algorithm (ie, weighted trimmed mean of M-values), implemented in edgeR³ R package (version 1.16.5). Afterward, we log-transformed the data and obtained precision weights using the voom function in the limma package.⁴ Finally, we performed a weighted fit using lmFit (also from limma) and the weights obtained from voom. To interrogate for IL15 and IL21 treatment effects in cell lines and ex vivo samples, we used a linear model with the following design: *Gene expression* \sim *Individual* + *Stimulation*, which captures the treatment effects on gene expression observed in the different cell lines and ex vivo samples analyzed. Likewise, in both cell lines and ex vivo samples, we used the same model to capture the effects of BNZ-2 in preventing IL15- and IL21-mediated effects. Nominal P values provided by lmFit were corrected for multiple testing using the Benjamini-Hochberg method. The results of these differential expression analyses are reported in [Supplementary Table 2](#). We considered a gene as differentially expressed between nonstimulated and stimulated samples if statistically supported at an FDR < 0.05.

Gene Ontology Enrichment Analysis

We used the Cytoscape app ClueGO (version 2.3.3)⁵ to identify gene ontology (GO) terms enriched among genes showing differentially expressed patterns on stimulation with the 2 cytokines or treatment with BNZ-2 in either cell lines and ex vivo samples (bulk-RNAseq). The following parameters were used when running ClueGO (unless otherwise stated): Min GO Level = 3; Max GO Level = 8; Minimum Number of Genes associated to GO term = 5; Minimum Percentage of Genes associated to GO term = 5. Enrichment P values were based on a hypergeometric test and we used Benjamini-Hochberg method for multiple testing correction. We identified 48 genes differentially expressed in response to IL21+IL15 combined treatment as compared with the treatment with IL15 alone ([Fig. 2B](#) and [C](#)) and classified them into 4 groups with respect to their change in expression on the addition of IL21 ([Fig. 2B](#)): (1) downregulation ($n = 1$), (2) decreased downregulation ($n = 6$), (3) upregulation ($n = 6$), (4) enhanced upregulation ($n = 35$). We performed GO enrichment analysis

considering only genes upregulated in response to both cytokines ($n = 41$, Fig. 2D). In ex vivo samples, we analyzed the bulk-RNAseq data and tested for GO enrichments among differentially expressed genes in response to individual treatment with IL15 ($n = 151$) and IL21 ($n = 12$) compared with untreated cells (Supplementary Figure 5E, Supplementary Table 4).

X-cell Analysis

To infer the cellular composition of the small intestinal epithelium isolated from human duodenal biopsies using a computation method, we compared the transcriptional profile obtained in ex vivo samples with those publicly available from distinct cell types (Supplementary Figure 5). We used the xCell tool,⁶ which applies 1822 pure human cell type transcriptomes from various sources. The input comprises a gene expression data set normalized to gene length, such as FPKM, which was obtained using Cufflinks.⁷ We excluded noncoding and lowly expressed genes with a mean FPKM < 1 across all in vitro and ex vivo samples combined, resulting in 12,726 genes.

Data Access

RNA-seq data generated in this study have been submitted to the National Center for Biotechnology Information Gene Expression Omnibus (<http://www.ncbi.nlm.nih.gov/geo/>) under the accession number: GSE120904

Flow Cytometry and Functional Assays

Directly conjugated antibodies were used to identify the following cell surface markers: TCR $\alpha\beta$ BV421, CD3 APC-Cy7, CD4 BV786, CD8 α BUV496, CD45 BV711, CD103 BUV395, sEPCam APC. For intracellular detection of phospho-STAT molecules, cells were fixed with 2% paraformaldehyde for 10 minutes at 37°C, washed, and stained for the following surface markers: CD45 (BD Biosciences), CD3 (Biolegend), and CD8 α (BD Biosciences), then permeabilized with Buffer III (BD Biosciences) and stained for pY705-STAT3 (Cell Signaling Technology) and pY694-STAT5 (eBioscience, San Diego, CA). Dead cells were excluded from the analysis using LIVE/DEAD Fixable 31 Aqua or LIVE/DEAD Fixable Near-IR (Thermo Fisher Scientific). CD8⁺ T cell lines or ex vivo single-cell suspensions from the epithelial compartment were stimulated, with or without BNZ-2, with the indicated concentrations of human recombinant cytokines (IL15, IL21, IL2) for 24 hours (before GzmB) or 48 hours (before Ki67 staining). After incubation, cells were stained with antibodies against surface receptors and with LIVE/DEAD fixable dye (Aqua; Thermo Fisher Scientific). For GzmB assessment, cells were permeabilized with Cytotfix/cytoperm fixation/permeabilization buffer (BD Biosciences) and incubated with monoclonal antibody against human GzmB (Life Technologies) for 30 minutes in 1X perm/wash buffer (BD Biosciences). To assess proliferation, cells were permeabilized with 1X Foxp3/Transcription Factor Staining Buffer Set (eBioscience) and incubated with monoclonal antibody against Ki-67 (BD Biosciences) for 60 minutes in 1X working solution of Permeabilization Buffer (BD Biosciences).

Samples were run on Fortessa X-20 cytometer and analyzed using FlowJo software version 10.2 (Tree Star, Ashland, OR).

Organ Culture

Three duodenal biopsies collected from 6 patients with active celiac disease were used for organ culture experiments (Supplementary Figure 9B). All 6 patients were enrolled at the University of Naples Federico II and diagnosed according to the ESPGHAN guidelines for celiac disease.⁸ Each duodenal bioptic fragment, villous surface facing upward, was placed on a stainless-steel mesh positioned over the central well of an organ culture dish. The biopsies were cultivated in RPMI 1640 (Sigma, Milan, Italy) medium supplemented with 15% fetal bovine serum (Life Technologies-GibcoBRL, Milan, Italy), 2 mM L-glutamine (Life Technologies-GibcoBRL), 100 U/mL penicillin, 100 μ g/mL streptomycin (Life Technologies-GibcoBRL), and 1 mg/mL insulin (Sigma) with or without 1 mg/mL of peptic-tryptic digest of gliadin (PTG) and 3 μ M of BNZ-2. Organ culture dishes were placed in a sterile anaerobic jar that was gassed with 95% oxygen and 5% carbon dioxide for 24 hours at 37°C. Supernatants were collected and stored at -80°C until downstream use. Soluble levels of IFN- γ were assessed in organ culture supernatants by Luminex Bead-based immunoassay platform (Assay Gate Inc., Ijamsville, MD). IFN- γ concentrations were determined by 5-parameter logistic regression algorithm with analysis of the median fluorescence intensity of each 8-point protein standard curve providing a larger range of quantitation than standard linear regression analysis. Analytical sensitivity or limit of detection was 0.1 pg/mL, whereas lower limit of quantification in human culture supernatants was 6.3 pg/mL.

Statistical Analysis

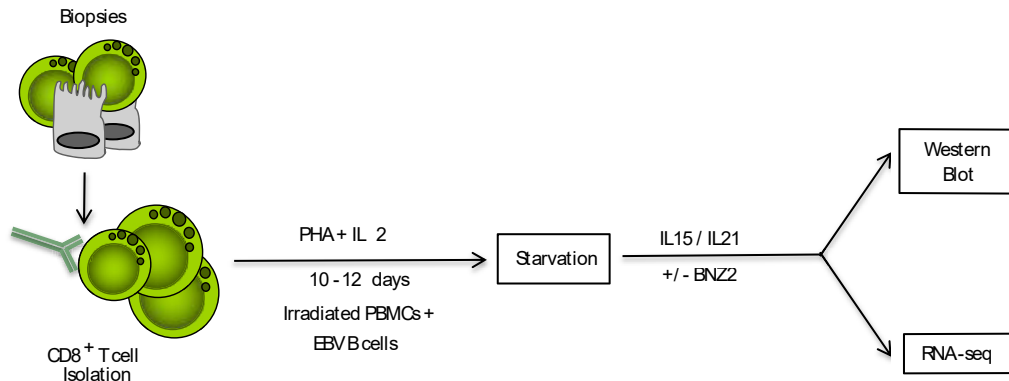
Pearson's test was used to evaluate correlation between *IL15Ra* and *IL21* transcript levels in small intestinal biopsies. Statistical comparisons for WB, PCR, flow cytometry, and organ culture experiments were determined by paired 1-way analysis of variance (ANOVA) test using GraphPad Prism software (La Jolla, CA).

NK Cell Proliferation Assay

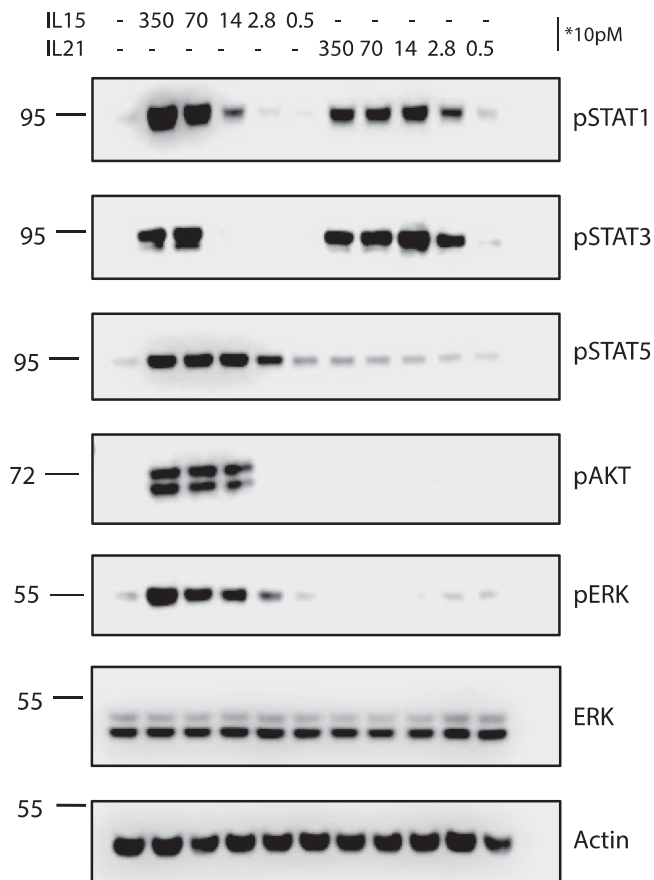
NK92 cells were cultured with 100 U/mL of human IL2 (Peprotech, Rocky Hill, NJ) in 10% fetal bovine serum (Gemini Bio, West Sacramento, CA), RPMI 1640 medium (Invitrogen, Carlsbad, CA) supplemented with 2 mM glutamine, penicillin, and streptomycin. Cells were withdrawn from IL2 overnight, plated in triplicate at a concentration of 0.2×10^6 cells/mL in 96-well plates and incubated, in presence or absence of 20 μ M BNZ-2, with human recombinant cytokines (Peprotech) IL15 at 77 pM, IL21 at 16 pM, IL2 at 67 pM, IL9 at 21 pM, and IL4 at 67 pM for 24 hours. Concentrations represent the EC50 for each cytokine for proliferation in this cell line. To quantify the rate of metabolically active cells, 20 μ L of WST-1 reagent (WST-1 Cell Proliferation Assay Kit by Clontech) was added for 6 hours before measuring the absorbance at 420 to 480 nm (Amax 450 nm).

Supplementary References

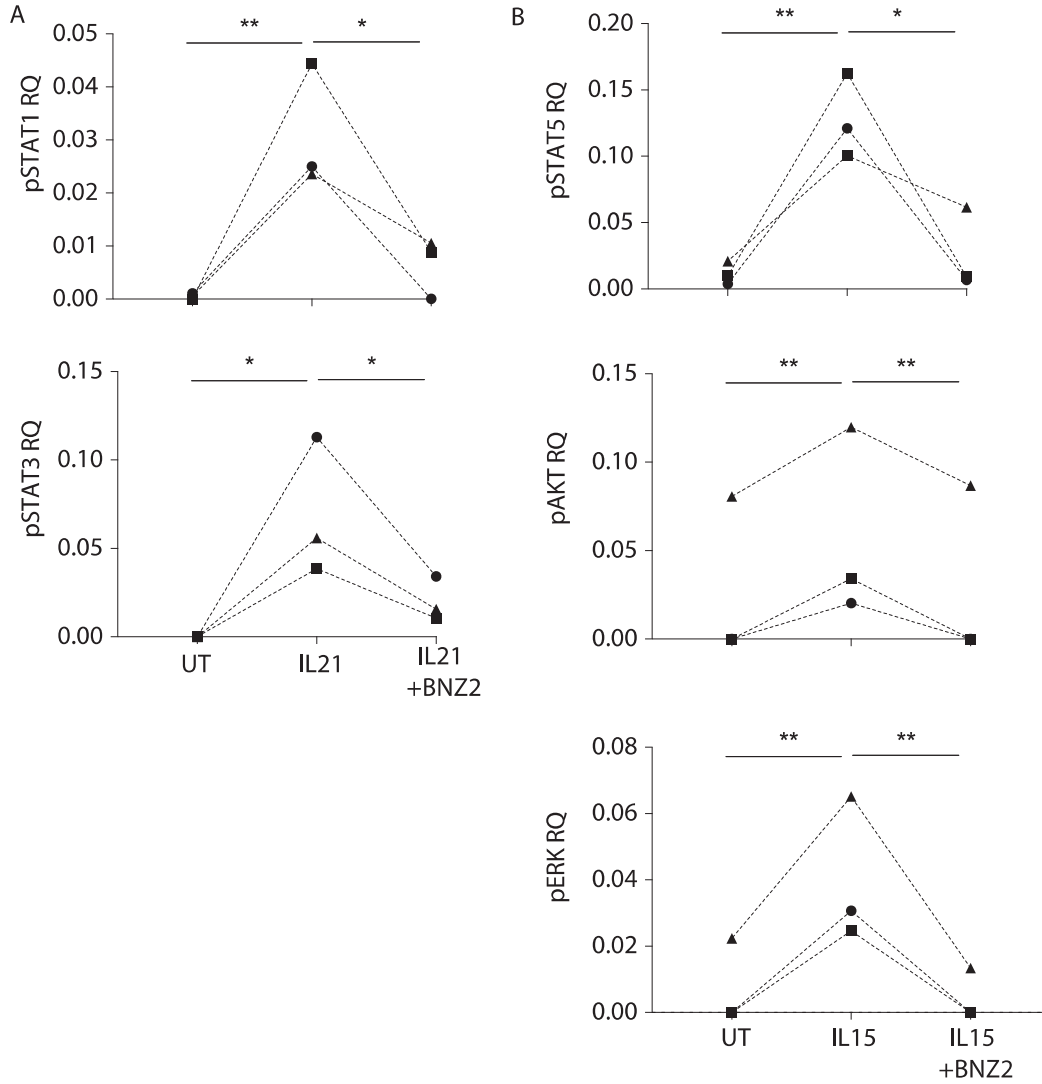
1. Kim D, Pertea G, Trapnell C, et al. TopHat2: accurate alignment of transcriptomes in the presence of insertions, deletions and gene fusions. *Genome Biol* 2013; 14:R36.
2. Anders S, Pyl PT, Huber W. HTSeq—a Python framework to work with high-throughput sequencing data. *Bioinformatics* 2015;31:166–169.
3. Robinson MD, McCarthy DJ, Smyth GK. edgeR: a Bioconductor package for differential expression analysis of digital gene expression data. *Bioinformatics* 2010; 26:139–140.
4. Ritchie ME, Phipson B, Wu D, et al. limma powers differential expression analyses for RNA-sequencing and microarray studies. *Nucleic Acids Res* 2015;43:e47.
5. Bindea G, Mlecnik B, Hackl H, et al. ClueGO: a Cytoscape plug-in to decipher functionally grouped gene ontology and pathway annotation networks. *Bioinformatics* 2009;25:1091–1093.
6. Aran D, Hu Z, Butte AJ. xCell: digitally portraying the tissue cellular heterogeneity landscape. *Genome Biol* 2017;18:220.
7. Trapnell C, Roberts A, Goff L, et al. Differential gene and transcript expression analysis of RNA-seq experiments with TopHat and Cufflinks. *Nat Protoc* 2012; 7:562–578.
8. Husby S, Koletzko S, Korponay-Szabó IR, et al. European Society for Pediatric Gastroenterology, Hepatology, and Nutrition guidelines for the diagnosis of coeliac disease. *J Pediatr Gastroenterol Nutr* 2012; 54:136–160.



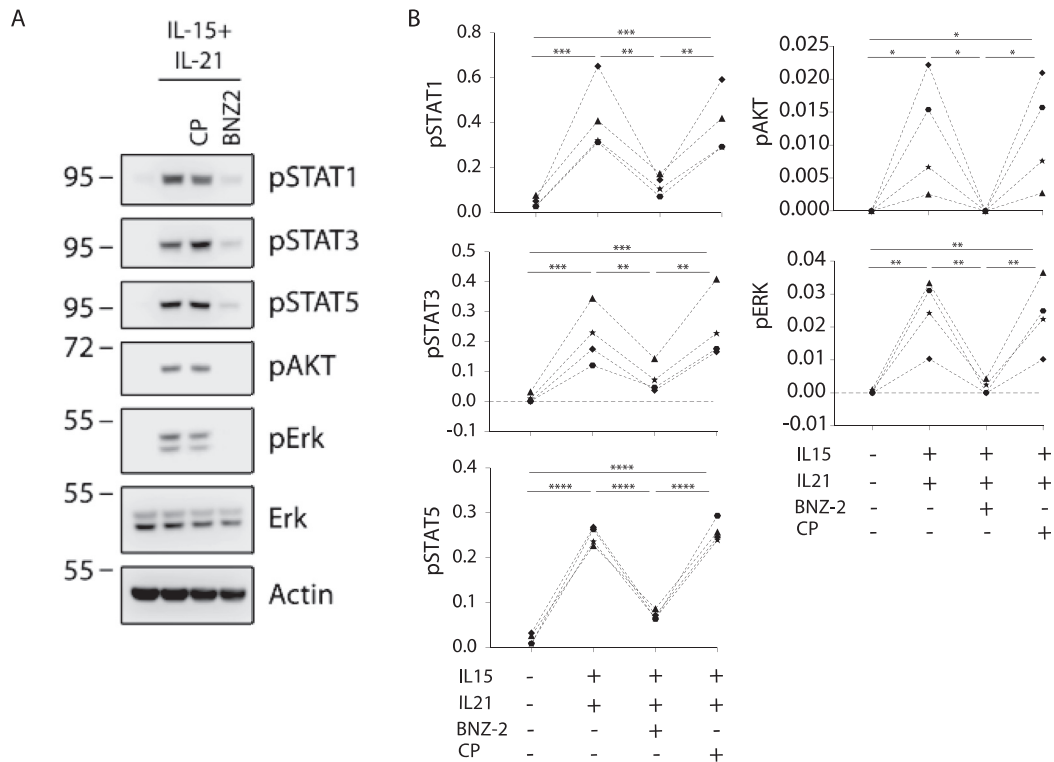
Supplementary Figure 1. Schematic of in vitro experiments in human primary intraepithelial CD8⁺ T-cell lines. Duodenal biopsies were processed to isolate the epithelial compartment as described in the Methods. CD45⁺CD103⁺CD3⁺CD8⁺TcR $\alpha\beta$ ⁺ cells were sorted from the epithelial fraction and cultured in presence of feeder cells, PHA, and IL2 for 10 to 12 days. Cells were deprived of IL2 (starvation) for 24 or 48 hours before cytokine stimulation (IL15 and/or IL21) in presence or absence of BNZ-2. WB was performed after 20 minutes of cytokine stimulation to look at phosphorylation of signaling molecules and RNA-seq after 2 hours of stimulation to investigate gene transcriptional profile.



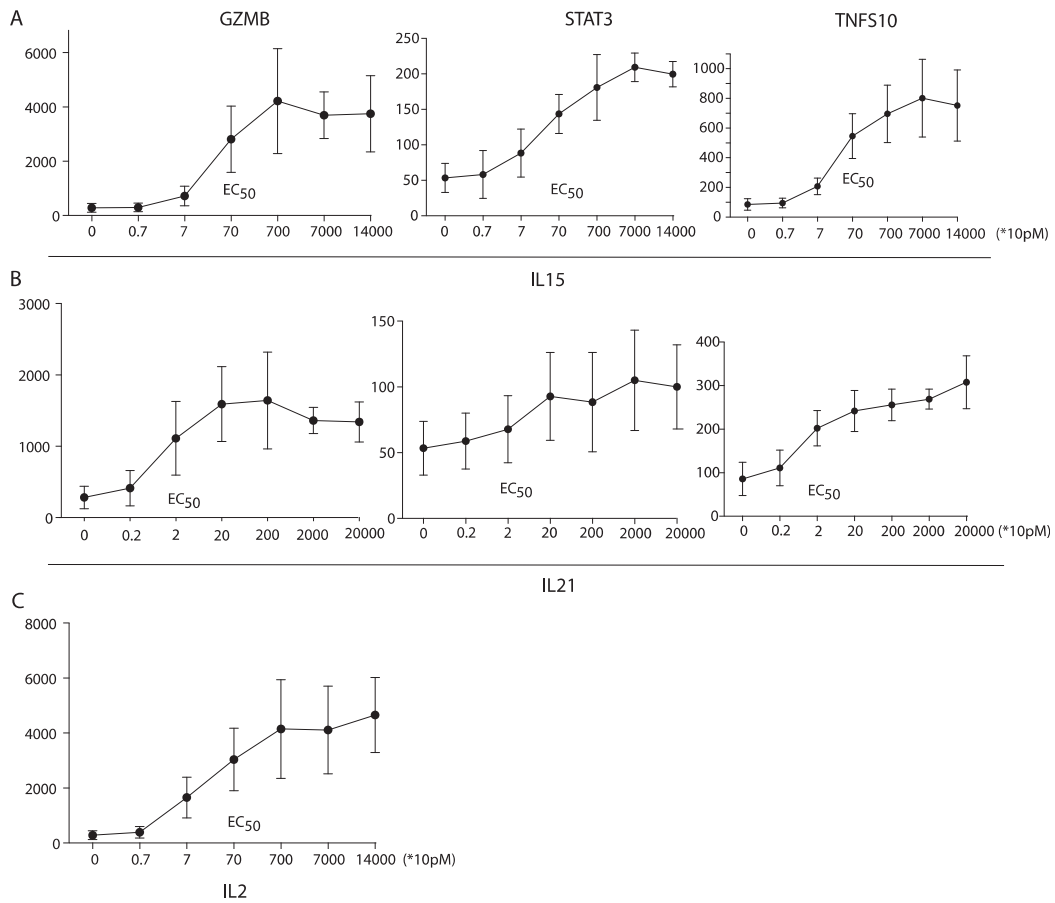
Supplementary Figure 2. Cytokine titration for signaling experiments. One representative of 2 WB showing phosphorylation of STAT molecules (pSTAT1, pSTAT3 and pSTAT5), AKT (pAKT), and ERK (pERK) in human primary short-term intraepithelial IE-CTL lines in response to increasing doses of human recombinant IL15 or IL21 (from 5 to 3500 pM). ERK and actin were used as equal loading controls.



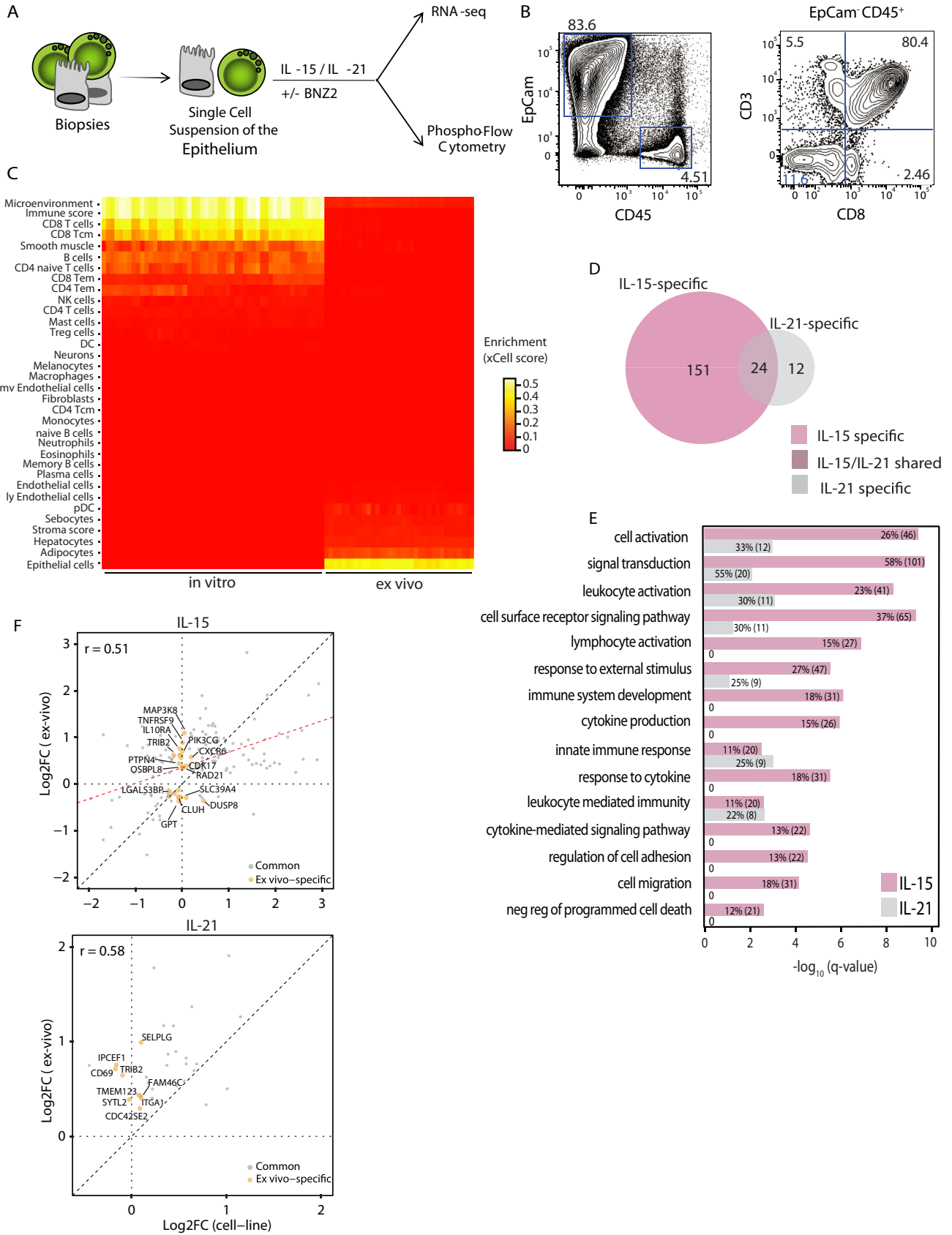
Supplementary Figure 3. BNZ-2 blocks distinct signaling pathways individually promoted by IL15 and IL21 in human IE-CTL. Quantification of 3 WB performed as in Figure 1C, showing protein levels of pSTAT1 and pSTAT3 in response to IL21 (14pM) treatment (A) and pSTAT5, pAKT and pERK in response to IL15 (140 pM) treatment (B), in absence or presence of 3 μM BNZ-2. Phospho-protein levels were normalized to averaged-ERK and actin as assessed by densitometry. Paired 1-way ANOVA was performed, **P* < .05, ***P* < .01.

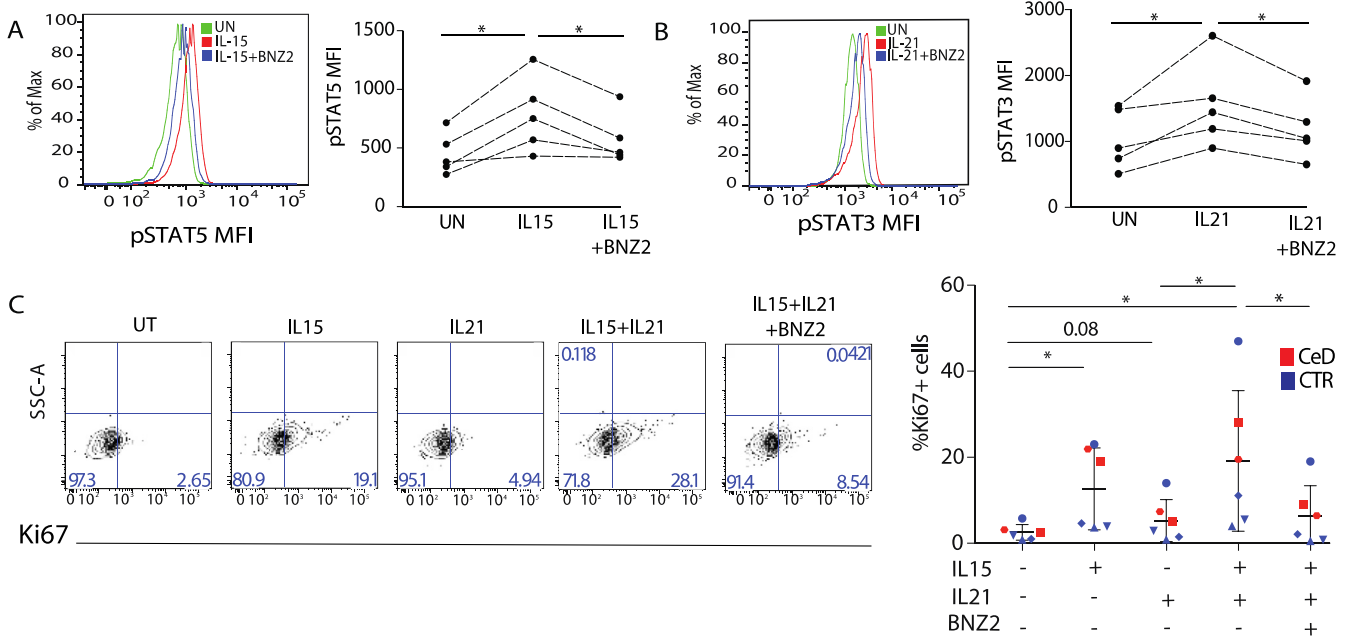


Supplementary Figure 4. BNZ-2, but not a control peptide, blocks cooperative signaling by IL15 and IL21. (A) One representative WB showing phosphorylation of STAT molecules (pSTAT1, pSTAT3, and pSTAT5), AKT (pAKT), and ERK (pERK) in human primary short-term IE-CTL lines in response to IL15 (140 pM) and IL21 (14 pM). ERK and actin were used as equal loading controls. (B) Quantification of 4 WB performed as in (A), showing protein levels of pSTAT1, pSTAT5, pAKT, and pERK in response to IL21 (14 pM) and IL15 (140 pM) treatment, in absence or presence of 3 μ M of BNZ-2 or a scrambled sequence of BNZ-2 used as a control peptide (CP). Phospho-protein levels were normalized to averaged-ERK and actin as assessed by densitometry. Paired 1-way ANOVA was performed, * $P < .05$, ** $P < .01$, *** $P < .001$, **** $P < .0001$.



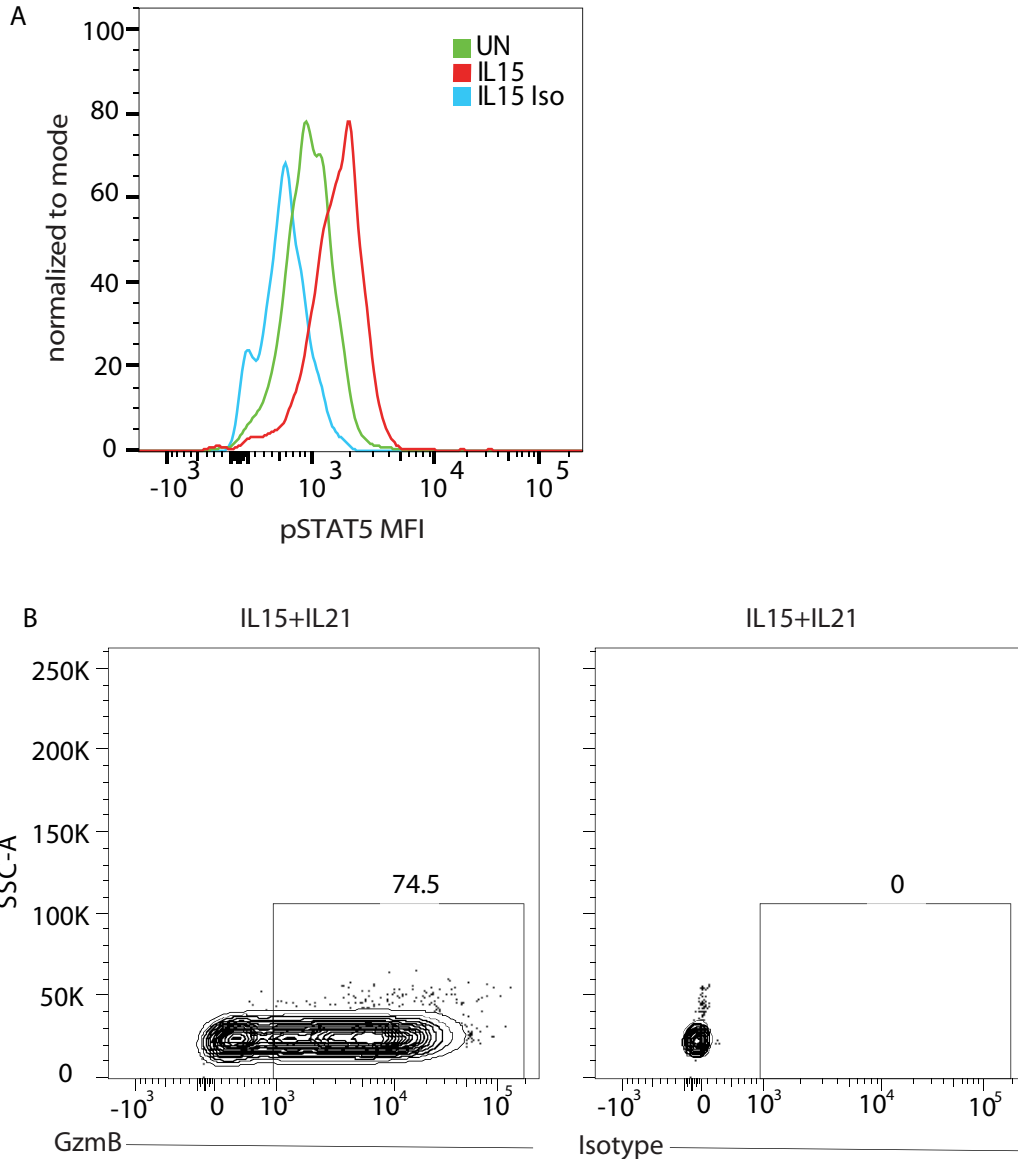
Supplementary Figure 5. Cytokine titration for transcriptional data. *GZMB*, *STAT3*, and *TNFS10* transcript levels relative to the housekeeping gene *GAPDH* are shown in response to increasing doses of (A) IL15 (from 7 to 140,000 pM), (B) IL21 (from 2 to 200,000 pM), (C) IL2 (from 7 to 140,000 pM). The EC50 is highlighted for each cytokine.



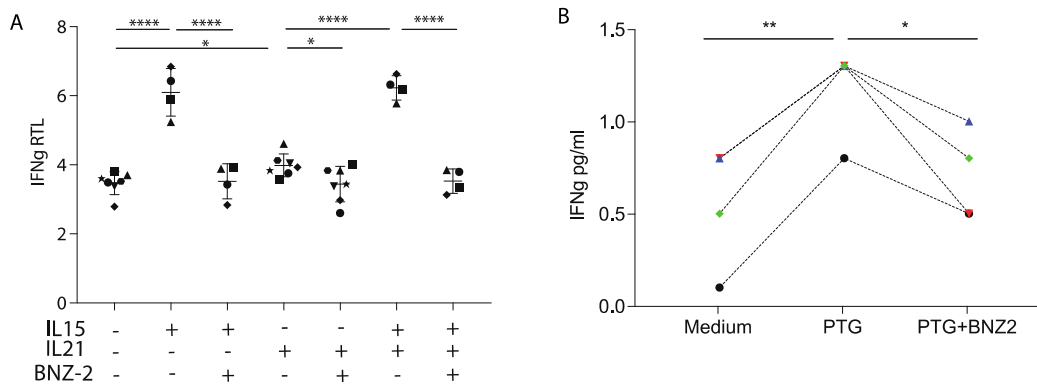


Supplementary Figure 7. BNZ-2 blocks IL15 and IL21 mediated effects on signaling and proliferation ex vivo. Mean fluorescence intensity (MFI) of pSTAT5 (A) and pSTAT3 (B) in response to IL15 (700 pM) and IL21 (20 pM) stimulation (red), respectively, as assessed by flow cytometry. The impact of 1 μ M BNZ-2 is shown (blue) and compared with untreated (UN, green). Quantification of 5 experiments from 5 control subjects is shown on the right. Paired 1-way ANOVA, * $P < 0.05$. (C) Representative FACS plots showing the frequency of Ki67-positive cells among Live CD3⁺CD8⁺ cells in response to IL15 (700 pM), IL21 (20 pM), and their combination with or without BNZ-2 (1 μ M). On the right: quantification of $n = 6$ experiments, including 2 patients with celiac disease (red), 1 potential and 1 on GFD, and 4 Controls (CTR, blue). Paired 1-way ANOVA, * $P < .05$. (A–C), a single-cell suspension of the small intestinal epithelial compartment was obtained from human duodenal biopsies and stimulated ex vivo with IL15 and/or IL21 in presence or absence of 1 μ M BNZ-2.

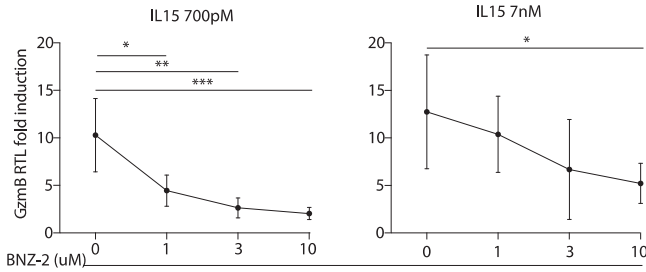
Supplementary Figure 6. Transcriptional changes in response to IL15 and IL21 stimulation ex vivo reveal a greater biological complexity of the ex vivo system. (A) Experimental layout of the ex vivo experiments. A single-cell suspension of the small intestinal epithelial compartment was obtained from human duodenal biopsies and stimulated ex vivo with IL15 and/or IL21 in presence or absence of 1 μ M BNZ-2. RNA-seq analysis was carried out to investigate gene transcriptional profile and phospho-flow-cytometry to look at phosphorylation of STAT3 and STAT5. (B) Representative flow cytometry showing percentage of CD45⁺EpCam⁻CD3⁺CD8⁺ T cells (range 1%–5%) and epithelial cells (EpCam⁺CD45⁻) in the small intestinal epithelial compartment. Gating included all nondebris events (FCS >25,000). Epithelial cells were CD45⁺ EpCam⁺, whereas, among EpCam⁻CD45⁺ cells, CD3⁺CD8⁺ cells were selected as IE-CTL. (C) Heat-map displaying the enrichment for distinct cell types in the ex vivo samples in comparison with cell lines, resulting from a computational enrichment analysis (X-cell). An overview of adjusted scores for 43 cell types in 259 purified cell type samples from Blueprint and ENCODE data sources. Most signatures clearly distinguish the corresponding cell type from all other cell types. (D) Venn-diagram showing DEGs on cytokine stimulation in the small intestinal epithelial compartment: 151 genes (dark gray) were deregulated in response to IL15, $FDR_{IL15} < 0.05$ and $FDR_{IL21} \geq 0.05$ (IL15 specific), 12 genes (light gray) in response to IL21 $FDR_{IL21} < 0.05$ and $FDR_{IL15} \geq 0.05$ (IL21 specific) and 24 genes (overlapping area) in response to both cytokines $FDR_{IL15} < 0.05$ and $FDR_{IL21} < 0.05$ (IL15/IL21 shared). (E) Histogram plot showing the impact of IL15 (700 pM) and IL21 (20 pM) stimulation on gene expression in comparison with untreated cells in the small intestinal epithelial compartment, as evaluated by GO enrichment analysis. Corrected P values (q-values) are shown on the x-axis. The number and rate (% above total genes) of genes contributing to each GO term is indicated for each cytokine stimulation. (F) Scattered plots displaying only IL15-specific (top) and IL21-specific (bottom) DEGs. Log₂FC in gene expression on cytokine stimulation (vs untreated cells) in cell lines (x-axis) and ex vivo (y-axis) is displayed. Each dot represents a gene, ex vivo-specific DEGs are in yellow. Correlation between gene expression levels in vitro and ex vivo is shown ($r = 0.51$ for IL15 and $r = 0.58$ for IL21, Pearson's). Data in (B–F) are based on expression levels assessed by RNA-seq in a single-cell suspension of the small intestinal epithelial compartment stimulated with cytokines in presence or absence of 1 μ M BNZ-2 ex vivo. $FDR < 0.05$ was the cutoff used to evaluate DEGs.



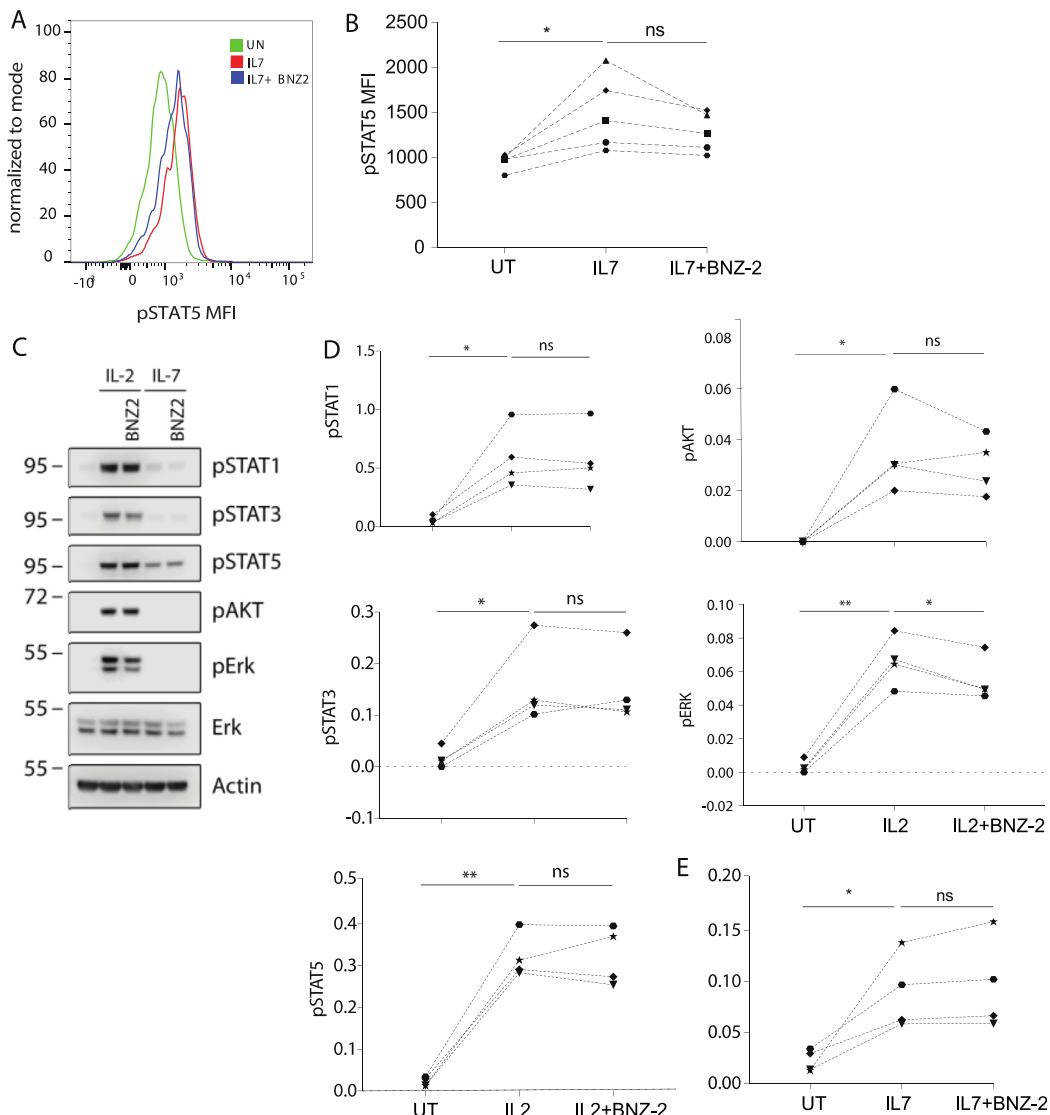
Supplementary Figure 8. Flow cytometry controls. pSTAT5 (A) and Granzyme B (B) staining and respective isotype controls as assessed by flow cytometry.



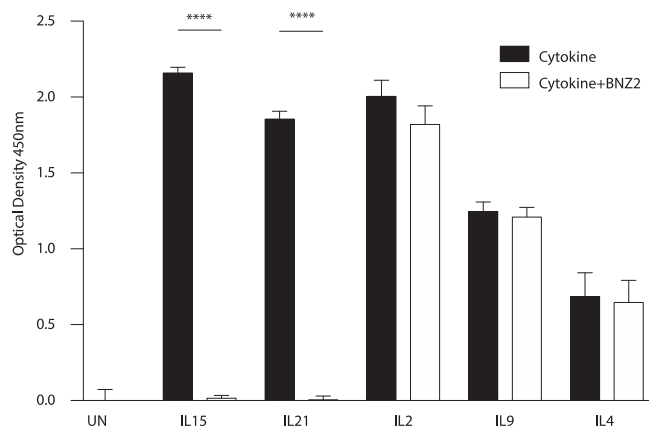
Supplementary Figure 9. BNZ-2 prevents IFN- γ production. (A) IFN- γ transcript levels relative to the housekeeping gene GAPDH (RTL) as assessed by qPCR in human short-term IE-CTL lines in response to stimulation with IL15 (700 pM) and/or IL21 (20 pM) in absence or presence of 1 μ M BNZ-2. Each distinct symbol shape refers to an individual cell line. (B) IFN- γ was detected by Luminex array in supernatants of small intestinal biopsies of patients with active celiac disease cultured in absence (Medium) or presence of 1 mg/mL of peptic-tryptic digest of gliadin (PTG) for 24 hours. The effect of BNZ-2 (1 μ M) on PTG-induced release of IFN- γ was quantified in supernatants of organ culture from 4 responsive subjects (each represented by a different symbol, shape, and color). Paired 1-way ANOVA was performed, * P < .05, ** P < .01, **** P < .0001.



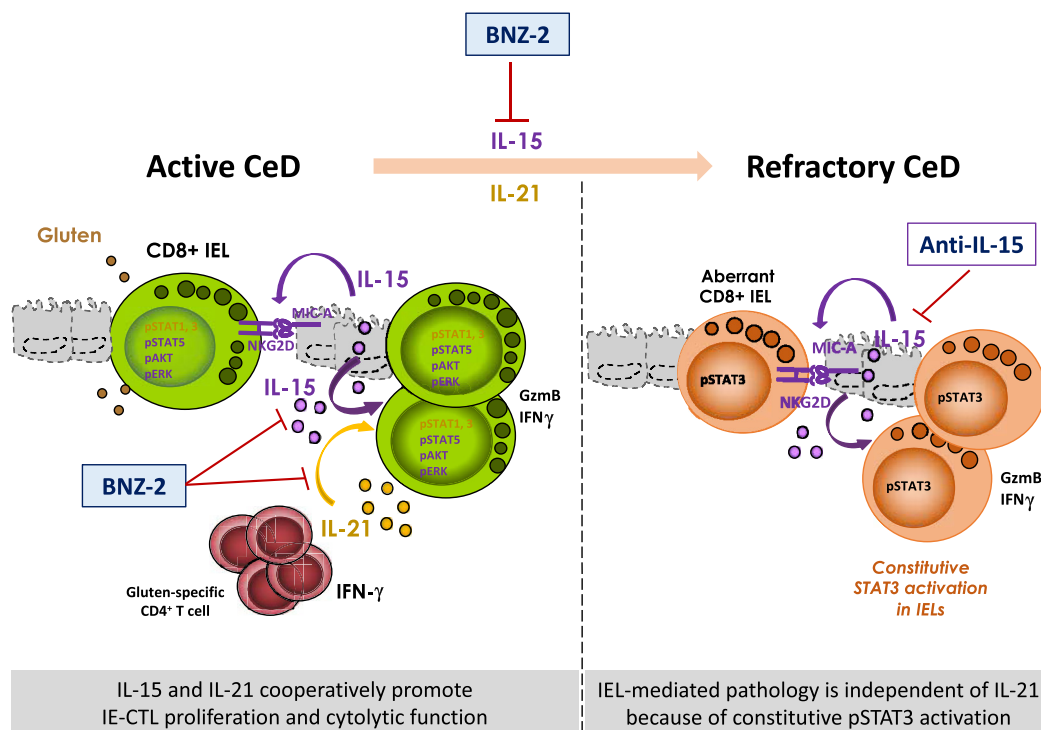
Supplementary Figure 10. BNZ-2 blocks IL15 in a dose-dependent manner. Dose-response of BNZ-2 to test its ability to mediate blocking of IL15 induced increase in Granzyme B (GZMB) expression. Fold increase of GZMB transcripts levels relative to untreated (UN) cells are shown in response to 700 pM (left) and 7 nM (right) of IL15. Paired 1-way ANOVA was performed, **P* < .05, ***P* < .01, ****P* < .001



Supplementary Figure 11. BNZ-2 impairs IL15, but not IL7 and IL2 mediated signaling. (A) Mean fluorescence intensity (MFI) of pSTAT5 was assessed by intranuclear flow cytometry in CD45⁺CD3⁺CD8⁺ IELs isolated ex vivo from 4 controls and 1 patient with celiac disease (same shape symbol refers to the same subject) in response to 700 pM of IL7 in absence or presence of 3 μM of BNZ-2. Fisher's exact test was performed; **P* < .05, ***P* < .01. (B) One representative WB showing phosphorylation of STAT molecules (pSTAT1, pSTAT3, and pSTAT5), AKT (pAKT), and ERK (pERK) in human primary short-term IE-CTL lines in response to IL2 (140 pM) or IL7 (140 pM) in absence or presence of 3 μM BNZ-2. ERK and actin were used as equal loading controls. (C) Quantification of 4 WB performed as in (B), showing protein levels of pSTAT1, pSTAT5, pAKT, and pERK. Phospho-protein levels were normalized to averaged-ERK and actin as assessed by densitometry. Paired 1-way ANOVA was performed, **P* < .05, ***P* < .01.



Supplementary Figure 12. BNZ-2 specifically impairs IL15 and IL21, but not other γ C cytokine-induced proliferation in NK cells. Proliferation of NK92 cells in response to different human recombinant γ C cytokines in presence or absence of 20 μ M BNZ-2. Cytokines were used at the following concentrations: IL15, 77 pM; IL21, 16 pM; IL2, 67 pM; IL9, 21 pM; and IL4, 67 pM, representing the EC50 for this cell line. The rate of metabolically active cells as assessed by WST-1 assay is represented as optical density of absorbance at 450 nm (OD450).



Supplementary Figure 13. BNZ-2 prevents development of villous atrophy and malignant transformation of IELs by blocking IL15 and IL21 signaling. Active celiac disease is characterized by the overexpression of IL15 and IL21 and tissue destruction mediated by CD8⁺ IE-CTL. IL21 (yellow) is produced by gluten-specific T cells (red) in the lamina propria, and promotes phosphorylation of STAT1 and STAT3 (in yellow in the nuclei), whereas IL15 (purple) enhances STAT5, AKT, and ERK (in purple in the nuclei) and contributes to STAT1 phosphorylation in IE-CTL. IL15 upregulates NKG2D, IL15 and IL21 cooperatively promote expansion, GzmB and IFN- γ production in IE-CTL. Furthermore, IL15 and IL21 promote the progression from Active to Refractory celiac disease. BNZ-2, by simultaneously blocking IL15 and IL21 in IE-CTLs, has the potential to alleviate tissue destruction and prevent progression to RCD and lymphomagenesis. In contrast, BNZ-2 has no advantage over anti-IL15 in patients with established RCD, where proliferation and activation of aberrant IELs (orange) is not dependent on production of IL21 by gluten-specific CD4 T cells, because of the acquisition of gain-of-function mutations in STAT3.